AD NUMBER: AD0068908
LIMITATION CHANGES
TO: Approved for public release; distribution is unlimited.
FROM: Distribution authorized to DoD Only; Administrative/Operational Use; Jul 1955. Other requests shall be referred to Army Chemical Corps, Biological Labs., Fort Detrick, MD.
AUTHORITY
USAMRMC ltr dtd 19 Oct 2017

DEPARTMENT OF THE ARMY
HEADQUARTERS, US ARMY MEDICAL RESEARCH AND MATERIEL COMMAND
AND FORT DETRICK
810 SCHREIDER STREET
FORT DETRICK, MARYLAND 21702-5000

October 19, 2017

Freedom of Information/
Privacy Act Office (Case 18-0001)

[redacted]

Dear [redacted]:

This letter responds to your electronic Freedom Of Information Act (FOIA) request dated September 29, 2017 addressed to FOIA@DTIC.mil and referred the US Army Medical Research And Materiel Command USAMRMC on October 5, 2017.

You requested "Release of document AD0068908, entitled, "Energetics Involvement In The Breakup of A Diverging Conical Jet".

USAMRMC is no longer responsible for the Chem/Bio/Nuc program but still has the responsibility for determining if it's appropriate for public release. Since this document is no longer sensitive in nature, the requested document is cleared for public release.

Fees associated with processing your request are waived in this instance.

Sincerely,

ROGERS.SANDRA.JEANNE.[redacted]

Digitally signed by ROGERS.SANDRA.JEANNE[redacted]
DN: c=US, o=U.S. Government, ou=DoD, ou=PKI, ou=USA, cn=ROGERS.SANDRA.JEANNE[redacted]
Date: 2017.10.19 12:29:03 -04'00'

Sandra J. Rogers
Freedom of Information Act/Privacy Officer
U.S. Army Medical Research and
Materiel Command

INTERIM REPORT 30

Energetics Involved In The Breakup Of A Diverging Conical Jet

CAMP DETRICK
FREDERICK MARYLAND

INTERIM REPORT 30

ENERGETICS INVOLVED IN THE BREAKUP OF A DIVERGING CONICAL JET

John S. Derr, Jr.

Work Completed September 1953

Munitions Division
Camp Detrick
Frederick, Maryland

Published July 1955

INTERIM REPORT 30

ENERGETICS INVOLVED IN THE BREAKUP OF A DIVERGING CONICAL JET

CONTENTS

FIGURES

CONTENTS, Cont'd

FIGURES, Cont'd

TABLES

ACKNOWLEDGMENTS

The author wishes to thank Mr. Roger Eyler, formerly of M Division, for assisting in the experimental work and Mr. Fred Kreissig, formerly of M Division, for his valuable assistance in designing the conical nozzle. Also, the author gratefully acknowledges the helpful suggestions and encouragement of Dr. Charles A. Boyd, formerly Chief, Applied Research Branch, M Division, and Dr. Ralph W. Hufferd, Deputy Chief, M Division. The author wishes further to express his appreciation for the constructive comments by Professor E. W. Comings and Dr. J. E. Myers of Purdue University.

SUMMARY

The average kinetic energy per unit volume required to produce breakup of a diverging, hollow conical liquid jet is measured as a function of viscosity, surface tension, and density of the liquid. An empirical equation relating the energy, called the "critical" energy, with the liquid properties is formulated. The "critical" energy is also measured as a function of nozzle design features using water as the liquid. A model is presented to explain the empirical relationship between "critical" energy and liquid properties. This model for the energetics involved in the breakup of the hollow conical jet is tentative. Some of the assumptions of energy partitioning used in formulating the model are being investigated as part of a continuing study in conical jet breakup.

INTERIM REPORT 30

BREAKUP OF A DIVERGING CONICAL JET

1. INTRODUCTION

Any complete description of the mechanism of aerosol production by nozzles should include some accounting of the partition of the energy initially available for the process. In the case of a single-fluid nozzle, the potential energy of the liquid is converted into kinetic energy in the closed hydraulic system where energy dissipation also occurs as a result of viscosity. Nozzles are usually designed so that divergence of streamlines occurs at the orifice, causing an increase in surface area per unit volume as the liquid flows from the nozzle in the atmosphere. Associated with this increase in surface area is an increase in surface energy of the liquid at the expense of its kinetic energy. This represents work performed against a potential gradient and therefore is conservative. The initial kinetic energy of the liquid will also be expended in two other ways:

1. Dissipation of kinetic energy will occur within the liquid as long as any velocity gradients exist there, and this energy will appear as heat. As long as velocity gradients initially set up in the nozzle exist, dissipation will result.

2. An exchange of momentum will take place between the liquid jet and the surrounding atmosphere, and the loss in kinetic energy of the liquid will appear in part as air motion and eventually as heat. Since this liquid-air interaction necessarily takes place at the surface of the liquid, the reaction of the air on the liquid will also tend to establish or maintain gradients in the liquid, causing or prolonging further dissipative loss.

Droplets comprising an aerosol produced by a single-fluid nozzle are formed by the breakup of thin sheets of liquid or rupture of fine filaments created in the sheet breakup, and if stability of the sheets is maintained, no droplets will be formed. Hence, one of the problems involved in the energetics of droplet production is the determination of the energy requirement necessary for sheet instability, and how the energy is expended in the process of producing this instability.

This report presents in part the results of some experimental work on the general problems of the energy requirement for breakup of a hollow conical jet. A hollow conical jet was chosen for two reasons. (1) At least two types of nozzles in use for the production of aerosols produce diverging hollow conical sheets of liquid, i.e., the impingement-type nozzle and the swirl-type nozzle. (2) The transition from stability to instability is easily recognized in the hollow conical jet from its shape.

The action of the jet can be qualitatively described as follows:

The hollow conical nozzle, shown schematically in cross section in Figure 1, produces a jet which will emerge from the nozzle at the angle, θ, to the axis. This expanding conical sheet will reach some maximum diameter consistent with the initial kinetic energy and physical properties of the liquid, and then will collapse under influence of surface tension into a solid stream. This phase of the nozzle behavior is stable and is shown schematically in Figure 2. As the initial kinetic energy is increased, a point is reached where collapse of the jet does not occur. At this point the conical sheet becomes discontinuous and surface tension cannot act to produce contraction of the jet. The liquid, having reached some maximum diameter, flows in a disrupted sheet parallel to the nozzle axis, i.e., zero angle between the jet surface and flow axis. See Figure 3.

This state will be referred to as the "critical state". Likewise, the initial velocity of the jet at the nozzle and the initial average kinetic energy per unit volume for this condition will be termed "critical velocity" and "critical energy".

As the initial kinetic energy is increased above the critical value, continued divergence of the jet takes place, and breakup of the jet will occur closer to the nozzle, as shown in Figure 4.

This report will treat the problem of the critical state and will be divided into three parts. Part 2 will examine the "critical energy" as a function of the liquid properties. Part 3 will describe experiments to determine "critical energy" as a function of nozzle design. Part 4 will consist of a simplified model for the energetics involved in the breakup of the hollow conical jet and will describe a preliminary experiment conducted to determine the energy partitioning.

2. EFFECT OF LIQUID PROPERTIES ON JET BREAKUP

A series of experiments was conducted to determine the "critical energy" for various liquids differing in density, surface tension and viscosity. To calculate the critical kinetic energy per unit volume, the flow rate of the nozzle under critical conditions and the annular area of the conical nozzle normal to streamlines must be known. "Critical energy" is defined by:

$$KE = \frac{1}{2} \rho \overline{v_c}^2 \qquad (1)$$

where $\overline{v_c}$ = average velocity of jet as it leaves the nozzle in the critical state

ρ = density of the liquid, assumed constant

KE = "critical energy" = average kinetic energy per unit volume, and from the equation of continuity, for constant density

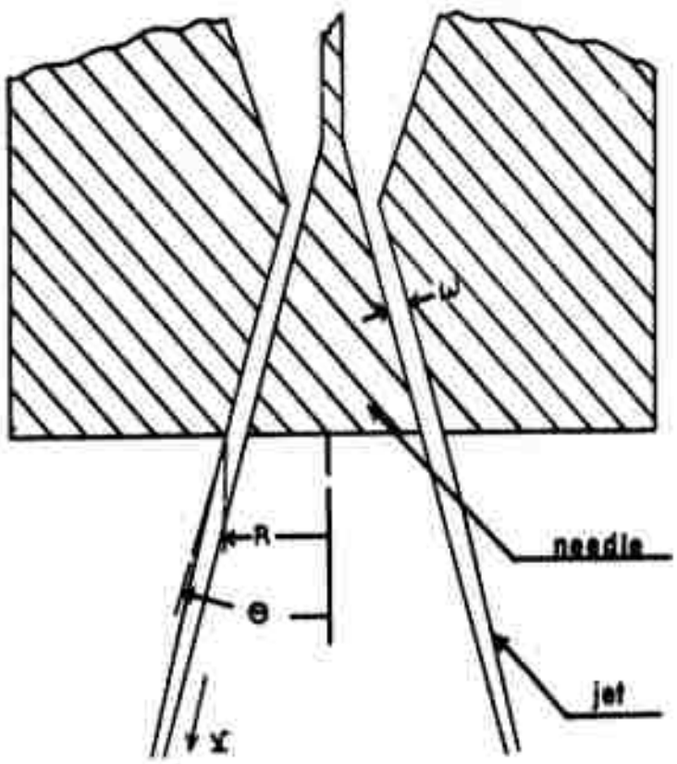

ω = annular separation

R = radius of nozzle base

θ = nozzle half-angle

V = jet velocity

Figure I. Hollow Conical Nozzle

NOZZLE BEHAVIOR OF JET WITH INCREASES IN KINETIC ENERGY

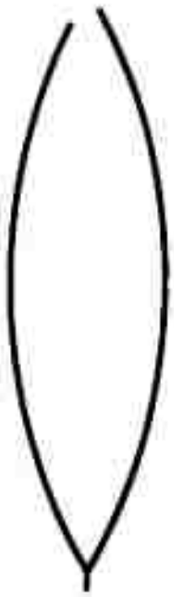

Figure 2. Stable

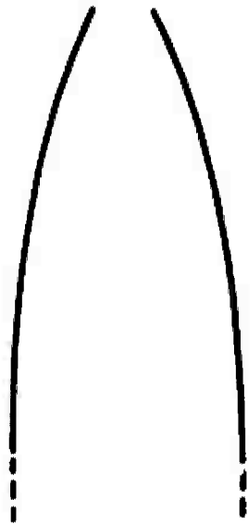

Figure 3. "critical state"

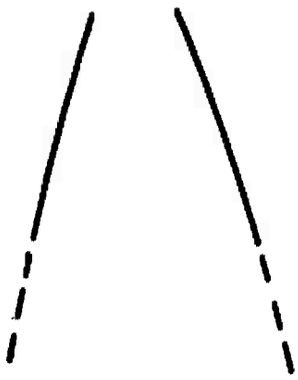

Figure 4. Above "critical state"

$$\overline{v_c}\ A_\perp = Q \qquad (2)$$

where $A_\perp$ = projected nozzle area, perpendicular to streamlines, assumed parallel to nozzle walls

Q = volume flow rate

The critical energy may be rewritten

$$KE = \frac{1}{2}\rho\left(\frac{Q}{A_\perp}\right)^2 \qquad (3)$$

The annular area, A is calculated from the nozzle geometry. The experimental nozzle is shown in Figure 5. The nozzle base is coupled to the upper portion or the nozzle with a 40-N micrometer thread. "O" rings in the piston portion of the nozzle provided an effective seal. The nozzle can be adjusted to any predetermined annular area by advancing the base from the closed nozzle position where contact is made between the centrally located rigidly fixed needle and the nozzle base. The area perpendicular to flow is given by:

$$A_\perp = \pi\left[\left(R - \frac{h^2}{r_1 \cos^2\theta}\right) + (R - r_1)\right]\sqrt{h^2 + \left[R - \frac{h^2}{r_1\cos^2\theta} - (R - r_1)\right]^2} \qquad (4)$$

where R = radius of the base orifice

θ = half angle of the nozzle

$r_1 = h \tan\theta$ = annular separation of the nozzle in its set position

h = vertical nozzle adjustment

The various liquids used in this series of experiments are listed in Tables I and II. Surface-tension measurements were made statically with a Dunoüy Tensiometer. Viscosity measurements were made with a rotational viscometer. Viscosities of these solutions were independent of shear rate and therefore classed as Newtonian. All measurements were made at the time of an experimental run, precluding temperature effects and effects of aging.

The experimental setup is shown in Figure 6. For a fixed nozzle setting, the nozzle pressure was adjusted until the critical velocity for the liquid under test was reached. The volume flow rate of the nozzle was then measured for the critical, steady-state condition. Three determinations of flow rate were made for each liquid, and liquid properties were checked after each run to determine the possibility of contamination. Average deviations for each run were between 1% and 3%.

TABLE I

Substance	Density	Surface Tension	Viscosity	Reynold's No.	Critical Energy	Ratio of Critical Energy & Surface Tension
	ρ $\frac{gms}{cm^3}$	σ $\frac{dynes}{cm}$	η centipoise	R_e	$\frac{1}{2}\rho\pi^2$ $\frac{ergs}{cm^3}$	$\frac{1}{2}\rho\pi^2/\sigma$
SERIES 1-NOZZLE 1						
Water	1.000	70.3	1.0	2129	1.34×10^6	1.88×10^4
Kerosene	0.800	29.0	1.8	714	0.750×10^6	2.58×10^4
Super Renuzit	0.785	27.0	1.0	1162	0.552×10^6	2.00×10^4
Mineral oil	0.850	34.0	45.0	67	3.98×10^6	11.7×10^4
50% Glycerol, H_2O	1.110	68.0	4.7	473	1.66×10^6	2.44×10^4
70% Glycerol, H_2O	1.160	64.0	12.2	305	4.45×10^6	6.95×10^4
10% Ethyl alcohol, H_2O	0.980	51.8	1.7	1052	1.27×10^6	2.45×10^4
20% Sucrose, H_2O	1.080	64.5	2.0	1067	1.55×10^6	2.41×10^4
SERIES 2-NOZZLE 2						
Water	1.000	72.0	1.0	1990	1.20×10^6	1.67×10^4
55% Sucrose, H_2O	1.235	71.1	12.5	288	3.92×10^6	5.50×10^4
80% Glycerol, H_2O	1.190	69.1	27.8	139	4.68×10^6	6.77×10^4
Mineral oil	0.855	33.8	44.5	64	3.51×10^6	10.4×10^4
Cenco hyvac oil	0.892	34.2	147.4	28	7.26×10^6	21.2×10^4
70% Glycerol, H_2O	1.145	66.7	11.9	295	3.36×10^6	5.02×10^4
Naphtha	0.755	27.0	1.1	555	0.43×10^6	1.59×10^4
Kerosene	0.815	29.5	2.0	536	0.57×10^6	1.93×10^4
60% Sucrose, H_2O	1.270	71.9	36.2	127	6.13×10^6	8.54×10^4
10% Ethyl alcohol, H_2O	0.985	51.3	1.6	1014	1.01×10^6	1.97×10^4

TABLE II

Substance	Density	Surface Tension	Viscosity	Reynold's No.	Critical Energy	Ratio of Critical Energy & Surface Tension
	ρ $\frac{ms}{cm^3}$	σ $\frac{dynes}{cm}$	η centipoise	R_e	$\frac{1}{2}\rho v_c^2$ $\frac{ergs}{cm^3}$	$\frac{1}{2}\rho v_c^2/\sigma$
SERIES 3 NOZZLE 3						
Kerosene	0.810	29.6	2.0	583	0.620×10^6	2.09×10^4
50% Glycerol by weight	1.150	58.5	5.3	513	1.96×10^6	3.35×10^4
10% Ethyl alcohol, H_2O	0.979	51.5	1.8	1247	0.996×10^6	1.933×10^4
Super Renuzit (Naphtha)	0.779	26.9	1.1	913	0.504×10^6	1.873×10^4
Tap water	1.000	72.0	1.0	1800	1.190×10^6	1.652×10^4
20% Sucrose, H_2O	1.065	67.0	1.9	1069	1.54×10^6	2.425×10^4
70% Glycerol, H_2O	1.170	59.6	14.2	283	6.460×10^6	10.838×10^4
50% Sucrose, H_2O	1.220	63.0	11.2	354	6.37×10^6	10.11×10^4
80% Mineral oil 20% Naphtha (wt.)	0.845	32.0	22.0	199	7.60×10^6	23.7×10^4
90% Mineral oil 10% Naphtha (wt.)	0.859	32.9	32.5	161	12.1×10^6	36.1×10^4
Dibutyl Phthalate	1.040	36.2	19.5	231	7.17×10^6	19.8×10^4
95% Mineral oil	0.859	32.9	43.0	132	14.4×10^6	47.0×10^4

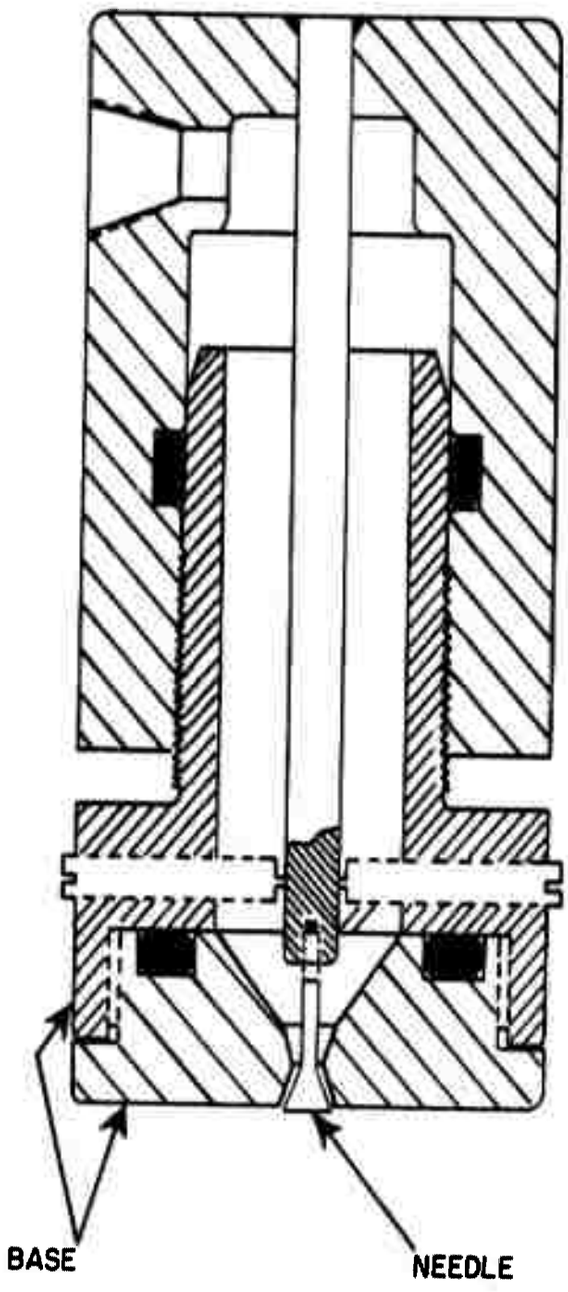

Figure 5. Experimental Nozzle

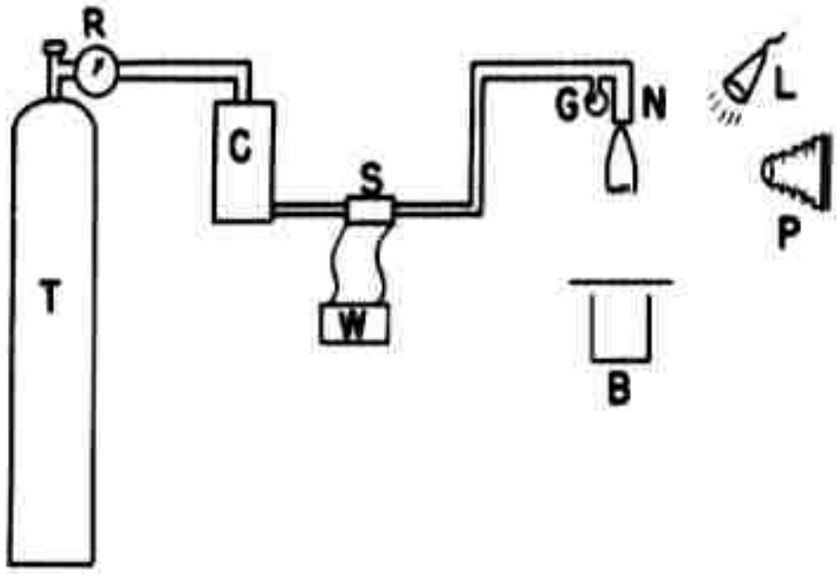

T – nitrogen tank
R – pressure regulator
C – liquid chamber
S – solenoid valve
L – flood lamp
W – timer
G – pressure gauge
N – nozzle
B – liquid sump
P – camera

Figure 6. Experimental Arrangement I

Three nozzles were used in this series of experiments, each with a 10-degree half angle and a 0.150" annular diameter at the nozzle exit. Nozzle No. 1 was constructed of brass with a bronze needle. Nozzle No. 2 was identical to nozzle No. 1 in design but was constructed with a stainless steel base and needle. The reason for this change in construction was two-fold: (1) to prevent surface corrosion and (2) to see if the machinability of the metal used in the nozzle construction could affect the nozzle performance. The needles in nozzle No. 1 and nozzle No. 2 protruded beyond the plane of the nozzle base with the nozzles in the adjusted position. Nozzle No. 3 was identical with Nozzle No. 2 except that the needle was shortened, so that there was no extension beyond the base.

Nozzle 1 and 2

Nozzle 3

Three sets of "critical energy" measurements were made, one set with each nozzle. Figure 7 shows results of the first experiment using nozzle No. 1. A plot is made of "critical energy" versus surface tension for the eight liquids tested. There are two points of interest about the plot. The "critical energy" appears to be an approximately linear function of surface tension for solutions with the lower viscosities. As the viscosity increases the "critical energy" values exceed those following the linear relationship. A viscosity effect is also reflected in the spread of values about the straight line average.

A second determination of "critical energy" as a function of liquid properties was made using nozzle 2. An additional number of high-viscosity solutions were included in the experiment as a check on the effect of high viscosity noted above. Results of this experiment corroborated the first. Higher viscosity solutions with the same surface tension required a higher initial average kinetic energy to reach the critical state than did the lower viscosity solutions. Results of this experiment are plotted in Figure 8.

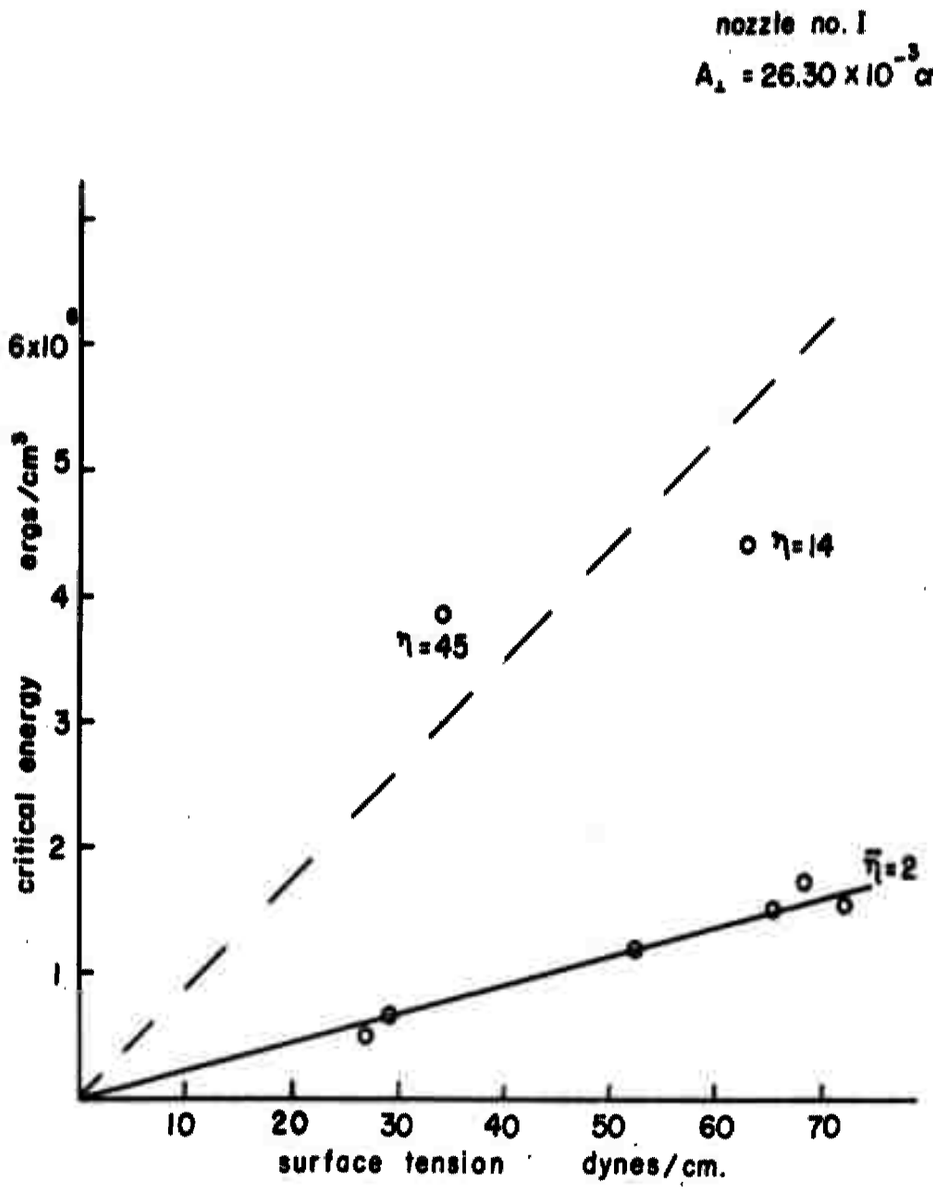

Figure 7. Critical Energy vs. Surface Tension, Nozzle I, Series I.

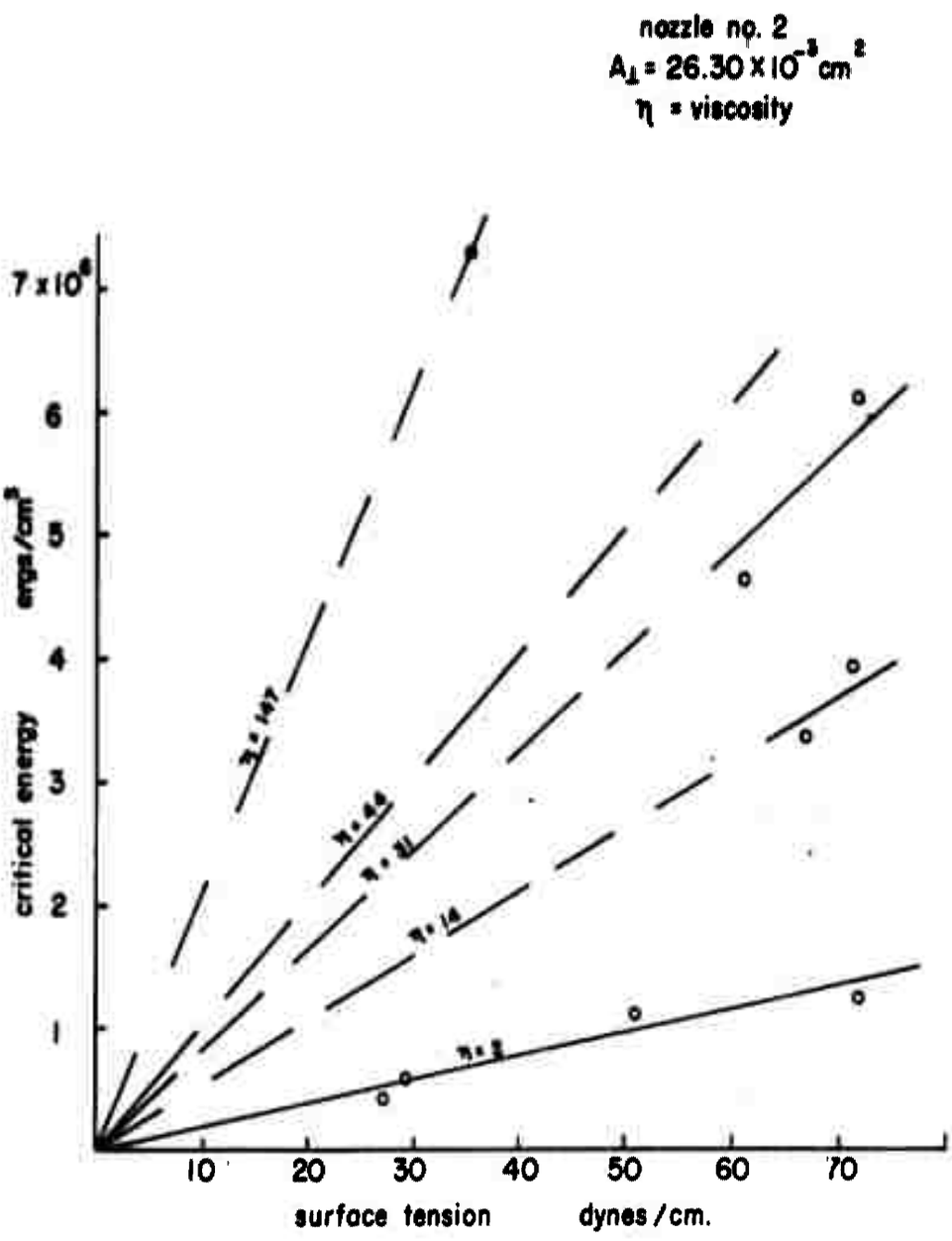

Figure 8. Critical Energy vs. Surface Tension, Nozzle 2, Series 2.

A final set of energy measurements was made using nozzle No. 3, which has the shortened needle. Results for the low-viscosity solutions were in general agreement with those using nozzles 1 and 2. However, energy requirement for the "critical state" with higher viscosity solutions was considerably greater. Results are shown in Figure 9.

The data indicate that the kinetic energy values plotted against surface tension might lie on a family of curves, where the parameter is viscosity. If the ratio of kinetic energy to surface tension is plotted against viscosity, a relationship is obtained as shown in Figure 10 for the data of series 3.

This data can be roughly approximated by two straight-line equations for two viscosity ranges.

$$\frac{\frac{1}{2}\rho \bar{v}_L^2}{\sigma} = k_1 \eta + C_1 \qquad 0 < \eta \leq 5 \text{ c.p.} \qquad (5)$$

$$\frac{\frac{1}{2}\rho \bar{v}_L^2}{\sigma} = k_2 \eta' + C_2 \qquad 5 < \eta < 45 \text{ c.p.} \qquad (6)$$

where $\eta' = \eta - 5$

η = viscosity, centipoises
σ = surface tension, dynes/cm
C_1, C_2, k_1, k_2 = constants

This indicates that kinetic energy as a function of surface tension can be expressed by a family of straight lines with slopes a function of viscosity.

$$\frac{1}{2}\rho \bar{v}_L^2 = k_1 \eta \sigma + C_1 \sigma \qquad \text{from (5)}$$

$$\frac{d\left(\frac{1}{2}\rho \bar{v}_L^2\right)}{d\sigma} = k_1 \eta + C_1 \qquad (7)$$

The straight-line relationship in Figures 7, 8, 9, for an average viscosity of 2 c.p. is one of a family of straight lines, with viscosity as the parameter.

The larger critical energy requirement for nozzle No. 3 is reflected in the value of K_2, which is higher than that for nozzles 1 and 2. See Figure 14.

Elimination of the free metal surface of the protruding needle of nozzles 1 and 2 has increased the stability of the jet, since for a given critical energy value for these nozzles, breakup has not yet occurred in nozzle 3. The value of k_2 is probably some measure of the jet stability.

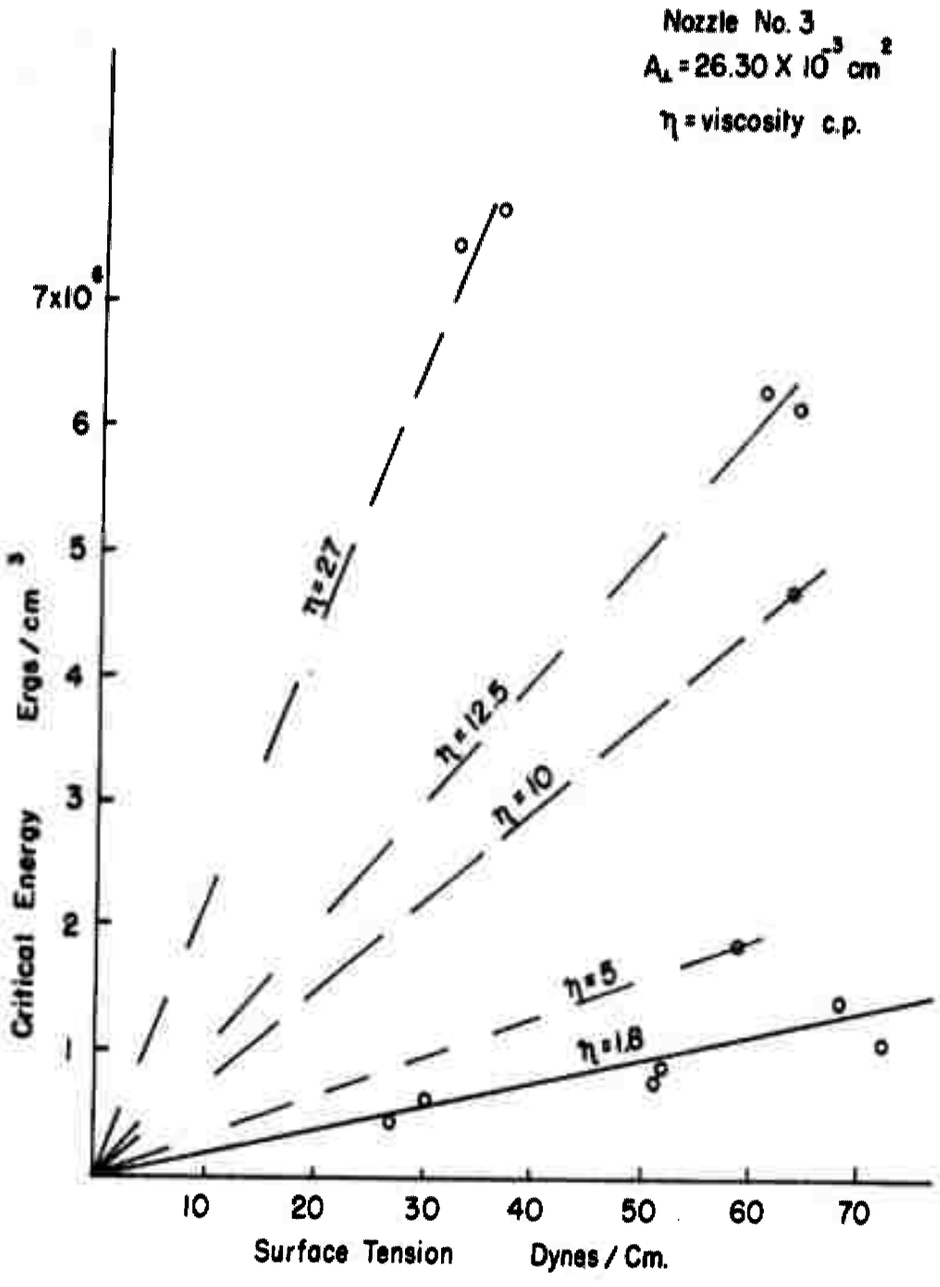

Figure 9. Critical Energy vs. Surface Tension, Nozzle 3, Series 3.

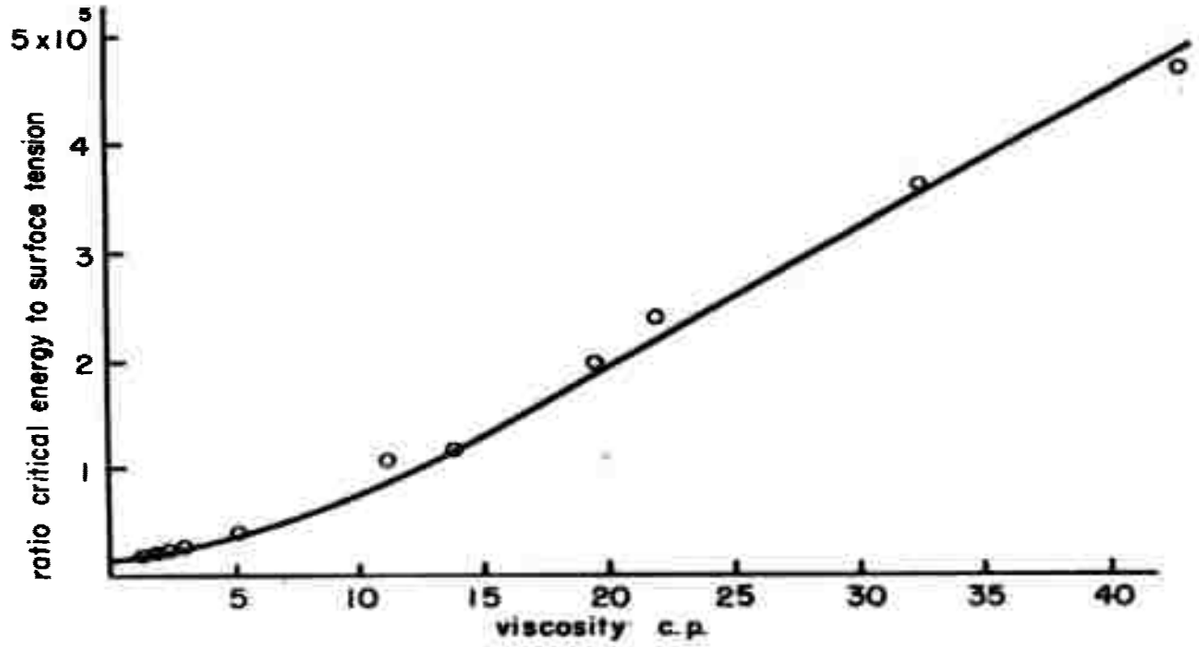

Figure 10. Kinetic Energy / Surface Tension Ratio Plotted Against Viscosity, Nozzle 3, Series 3.

The critical energy appeared to be independent of the Reynold's Number for the low-viscosity range. Reynold's Number was computed using the "hydraulic mean depth", defined as the ratio of area to wetted perimeter of cross section. Its use is based on the assumption that, for a given area, the resistance to flow depends upon the amount of fluid in contact with the surface. For the high-viscosity range, critical energy appeared to be a decreasing function of Reynold's Number. The value of the Reynold's Number in this region depends strongly on viscosity, and the apparent dependence of critical energy on Reynold's Number probably reflects its dependence on viscosity. Figure 11.

The two straight-line regions given by equation 5 and 6 may possibly represent two conditions of jet stability. And the transition between the two can be characterized by a fixed value for the Reynold's Number. Figure 12 shows the critical energy as a function of Reynold's Number. Critical energy is independent of Reynold's Number for a value of $R>500$. Figure 13 is a plot of critical energy versus viscosity and a discontinuity is found at a viscosity of approximately 5 cp. Figure 14 shows the empirical plot of equations (5) and (6) and the transition takes place at $n\approx 5$ cp, corresponding to a Reynold's Number of ≈ 500 as shown by Figure 11.

The ratio of critical energy to surface tension when plotted against Reynold's Number gives evidence of a discontinuity at $500< R_c <600$. For values of $R_c>500$, the ratio is independent of R_c, whereas for $R<500$ the ratio is dependent on R, reflecting the dependence of R on viscosity in this region. See Figure 15. Hence, $R_c\approx 500$ may represent the transition between two regions of jet stability and the transition may be from a condition of turbulent to laminar flow in the nozzle.

Summary of Part 2

1. The average kinetic energy per unit volume necessary to produce breakup of the expanding conical jet is a function of viscosity and surface tension.

2. The dependence of this "critical energy" on viscosity is probably due to three factors:

   (a) Viscous loss in energy due to velocity gradients in the liquid.

   (b) Inherent stability of the jet as a result of type of flow through the nozzle.

   (c) Stability of the jet as a result of the damping of disturbances which might otherwise have a disrupting effect. Increased stability would enable more work to be performed both in storing surface energy and in working against friction.

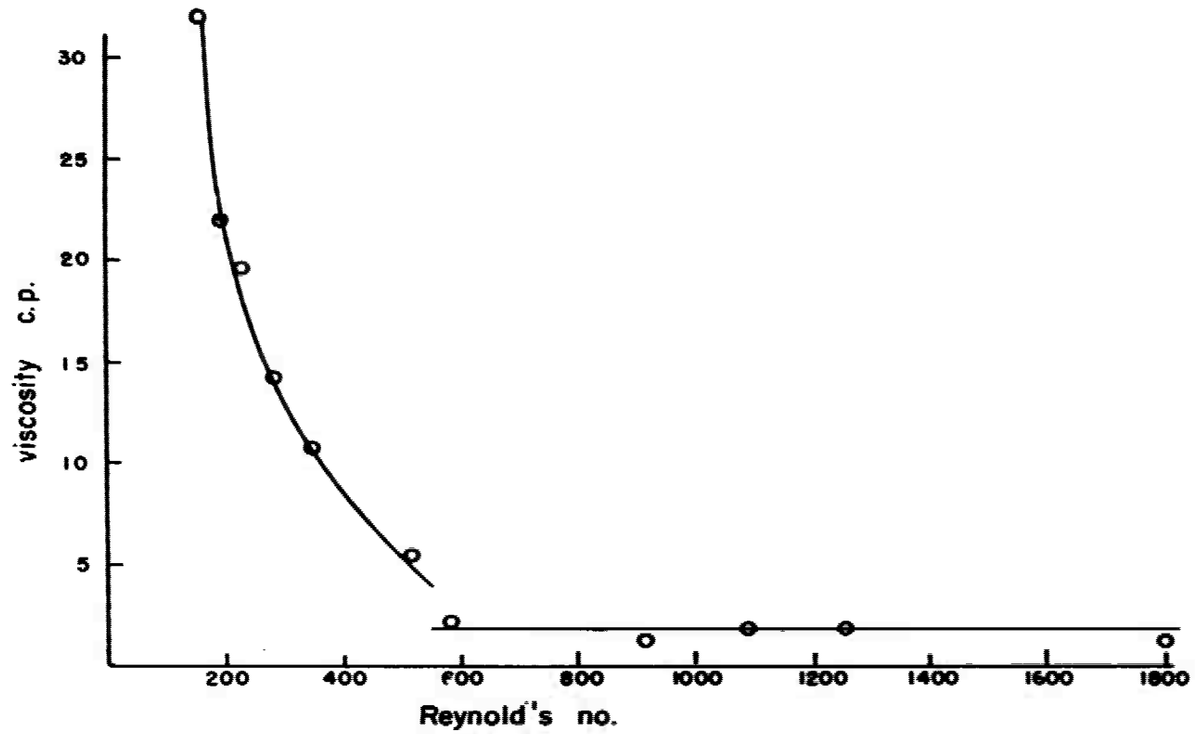

Figure 11. Relationship Between Viscosity and Reynold's Number.

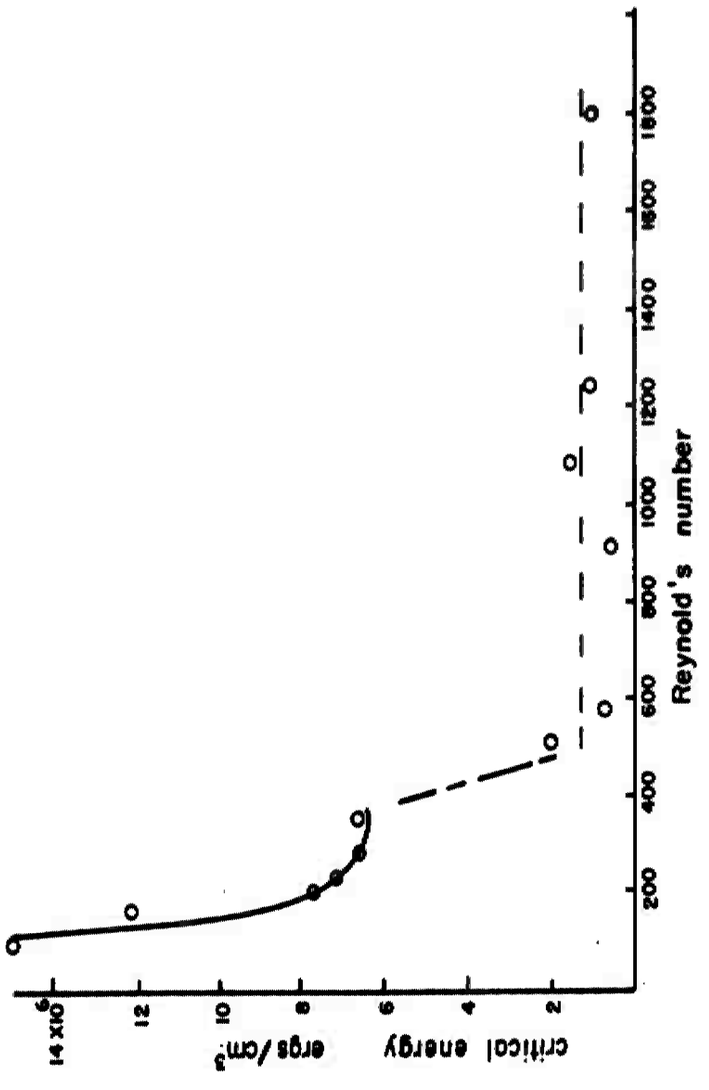

Figure 12. Critical Energy As A Function of Reynold's Number.

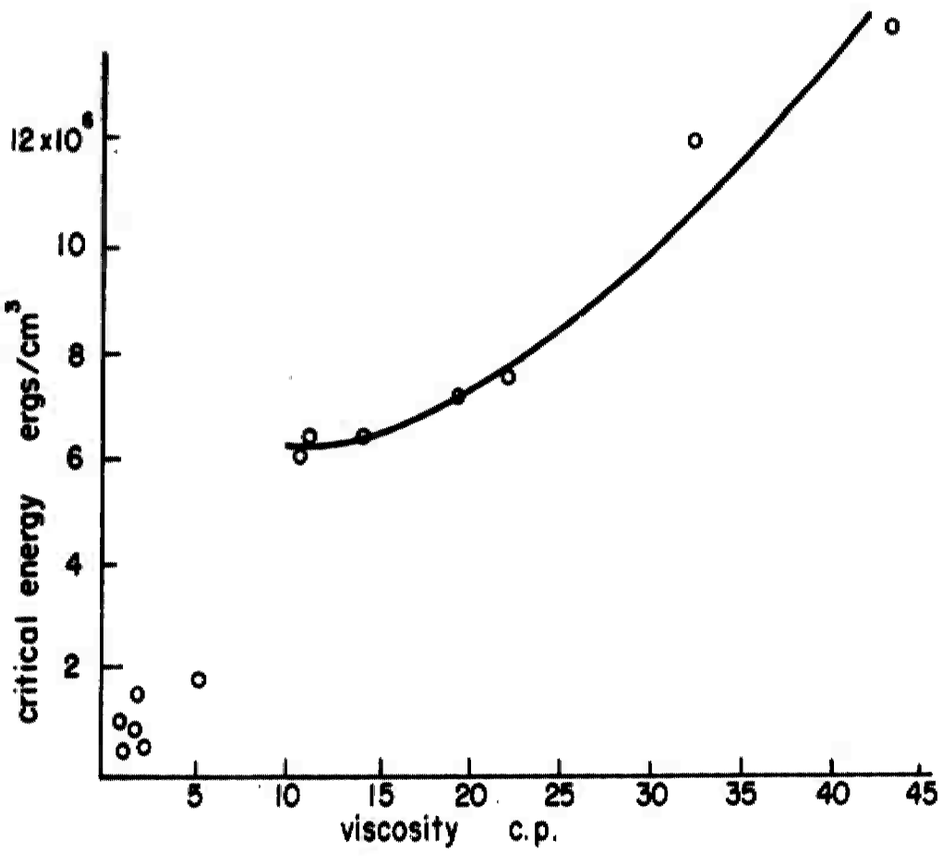

Figure 13. Critical Energy vs. Viscosity.

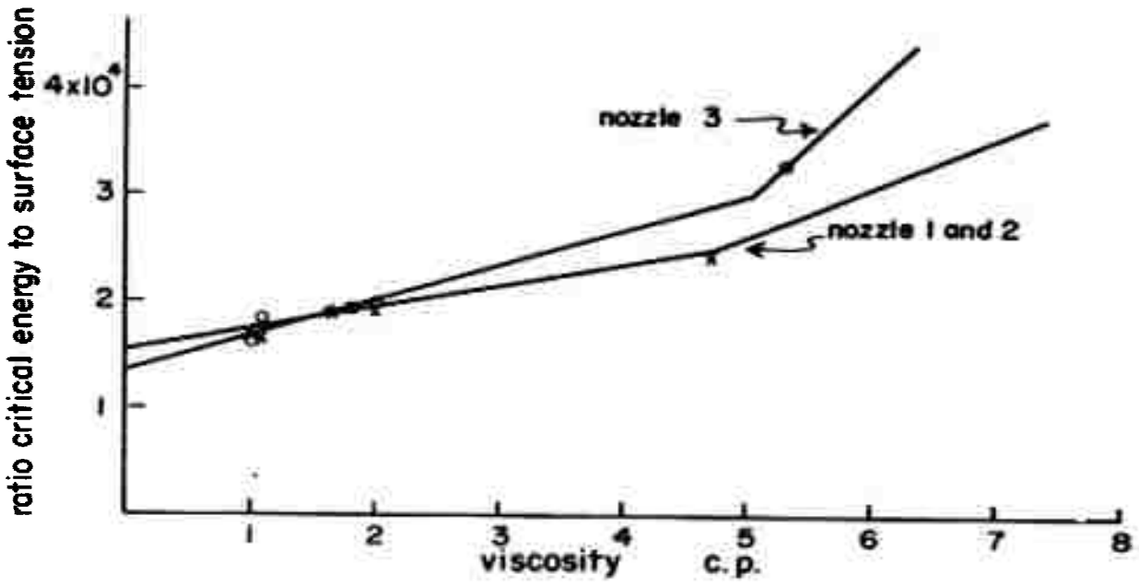

Figure 14. Empirical Plot Of Two Straight-line Equations For Two Viscosity Ranges [Equations (5) and (6)].

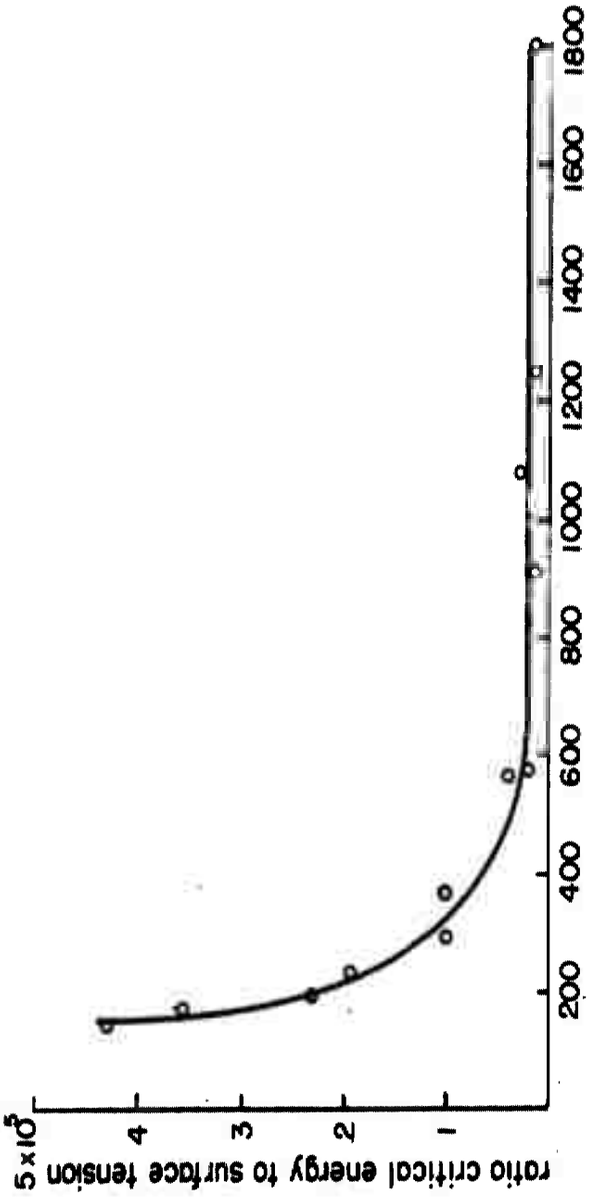

Figure 15. Critical Energy / Surface Tension Ratio Plotted Against Reynold's Number.

3. EFFECT OF SOME ASPECTS OF NOZZLE DESIGN ON JET BREAKUP

A series of experiments was performed to correlate "critical energy" with the following conical nozzle design features:

1. Radius of nozzle annulus, R
2. Width of nozzle annulus, ω
3. Nozzle angle, θ

These features are shown in Figure 1.

Two values were chosen for each parameter, resulting in eight different combinations. This required the machining of four nozzle bases and four needles, and afforded a two-point plot of "critical energy" versus a given design feature, with the remaining two serving as parameters.

Other apparatus included a Sylvania RA-210 high-speed flash source with an approximate 4-microsecond flash duration, a strobe unit, and a 45° aluminum sector mounted on a variable-speed motor. This equipment was used in photographing the conical jets and in determining jet velocity. Distilled water was used as the test liquid.

The experimental arrangement for this series of experiments is shown schematically in Figure 16. The position of the nozzle was adjusted so that the point of breakup of the jet in the critical state lay in the plane of the horizontally mounted aluminum sector. With this adjustment made, the sector was rotated by the variable-speed motor and allowed to "chop" the jet in the critical state at the point of breakup. The angular velocity of the sector was measured stroboscopically during this sectoring process, and a high-speed flash photograph was taken. Illumination was triggered by the sector as it passed through the jet. A second photograph was made of the jet in the critical state without its being sectored. Volume flow rate as a function of pressure was measured for each nozzle, and the critical volume rate of flow was determined from the photographically recorded nozzle pressure at the critical state of the jet.

The critical energy was defined as in Part 2, the area of the nozzle annulus perpendicular to the flow being calculated from the nozzle geometry. Results of critical energy determination as a function of nozzle design features are plotted in Figure 17. In general, the critical energy decreased with increased angle, annular width, and annular diameter for each nozzle. The dependence of critical energy on angle was more marked than its dependence on other design features.

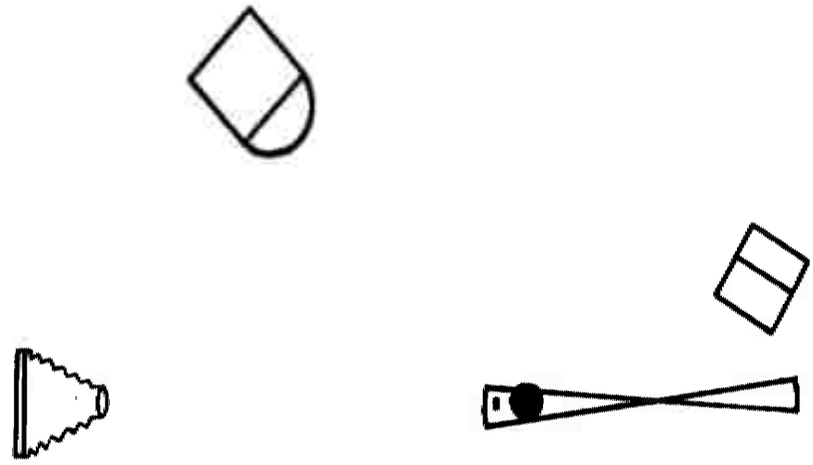

TOP VIEW

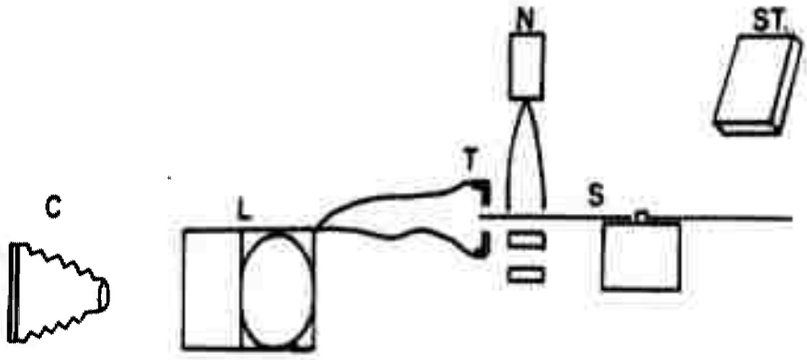

C – camera
L – high speed flash
T – trigger contact
N – nozzle
S – sector
ST – stroboscope

FRONT VIEW

Figure 16. Experimental Arrangement II

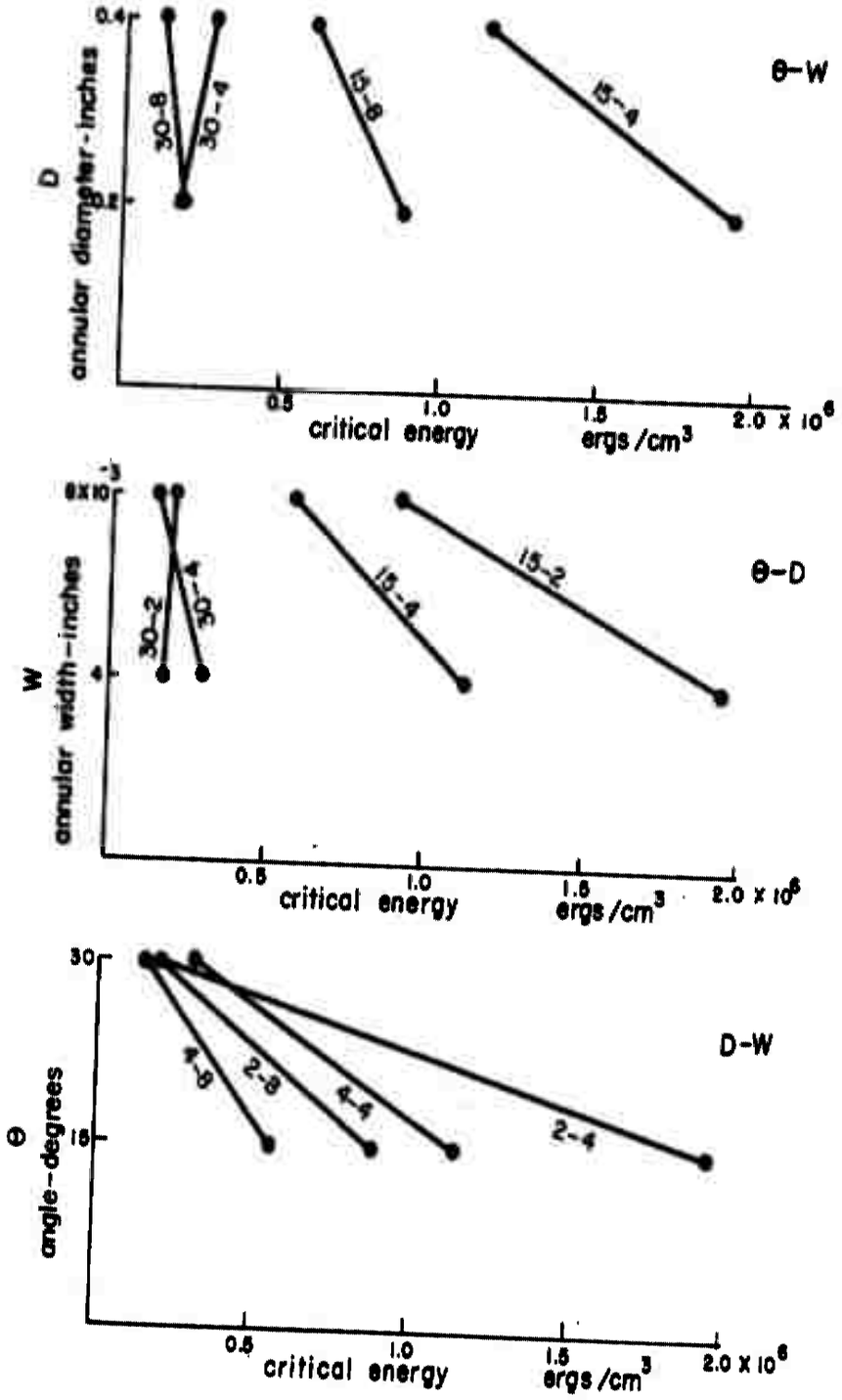

Figure 17. Critical Energy Determination As A Function Of Nozzle Design Features.

A measure of the thickness of the conical sheet at point of breakup was obtained from photographs of the interrupted jets. The velocity of the jet was calculated by using the rotational velocity of the rotating sector and a measurement of the interrupted jet from the photograph according to:

$$V_a = \frac{L \cdot 45}{360 \cdot f}$$

where V_a = apparent jet velocity cm/sec

f = rotational frequency cycles/sec

L = interrupted jet length, cm.

Also, the diameter of the jet at point of breakup was determined from the photographs, and from the equation of continuity the apparent thickness of the conical sheet could be determined.

$$t_a = \frac{Q \cdot 45}{\pi d L \cdot 360 \cdot f} \qquad (8)$$

where Q = volume flow rate, cm^3/sec.

d = jet diameter, cm.

t_a = apparent jet thickness.

Results of this determination are plotted in Figure 18. The apparent sheet thickness decreases with increased angle and increases with increased nozzle diameter and annular width for each nozzle.

The values of the apparent sheet thickness were all of the same order of magnitude, the average value being 3.49×10^{-3} cm $\pm$ 0.70×10^{-3} average deviation. In the calculation of sheet thickness from the measured jet velocity, a uniform circular annulus was assumed, which in practice was not the case, since surface irregularities did exist. Hence, the term "apparent" is used to express the thickness the sheet would have had if the cross-sectional area had been regular.

The sheet thickness at breakup can be related to the critical energy by an expression for conservation of energy. If one assumes that the kinetic energy due to the horizontal or radial component of velocity of the liquid per unit volume at the nozzle is expended in storing surface energy and in doing non-conservative work, the following expression can be written:

$$\frac{1}{2} \rho \bar{V}^2 \sin^2\theta = 2\sigma \left(\frac{1}{T_2} - \frac{1}{T_1} \right) + \int F \, dx \qquad (9)$$

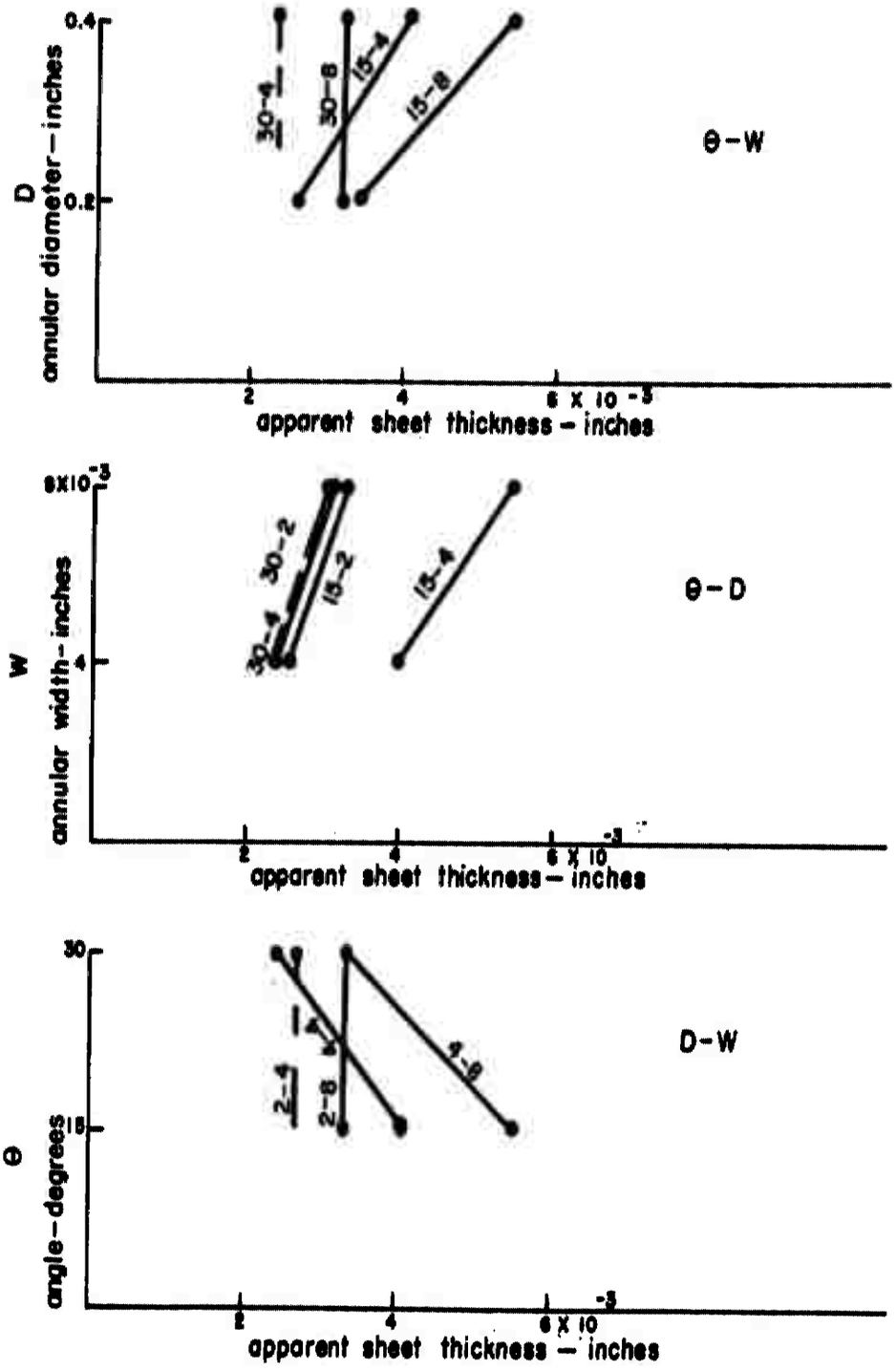

Figure 18. Relationship Of Apparent Sheet Thickness To Nozzle Design Features.

where θ = half angle of the nozzle

T_1 = initial sheet thickness

T_2 = final sheet thickness

$\bar{V}$ = initial critical velocity

σ = surface tension

$\int F \cdot dx$ = term expressing dissipative loss in energy in horizontal direction.

There is no term on the right side of equation (9) involving kinetic energy, since at point of breakup the radial component of velocity is zero. See below..

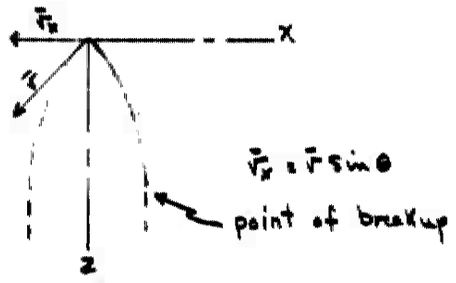

From equation (9), an expression can be written which will characterize each combination of nozzle design features. The ratio of the change in surface energy to the initial kinetic energy available for this conservative work will be called "nozzle efficiency", and will be a measure of the efficiency of the nozzle in producing a transformation of kinetic energy to surface energy per unit volume.

$$E = \frac{2\sigma\left(\frac{1}{T_2} - \frac{1}{T_1}\right)}{\frac{1}{2}\rho \bar{V}^2 \sin^2\theta} = 1 - \frac{\int F \cdot dx}{\frac{1}{2}\rho \bar{V}^2 \sin^2\theta} \qquad (10)$$

E = "nozzle efficiency"

These "nozzle efficiency" values are plotted in Figure 19. The dependence on angle is again, as in the case of critical energy, stronger than the other design features.

The dissipative term in Equation (9) affects the nozzle efficiency and results from:

(1) velocity gradients in the sheet

(2) interaction of the sheet with the atmosphere.

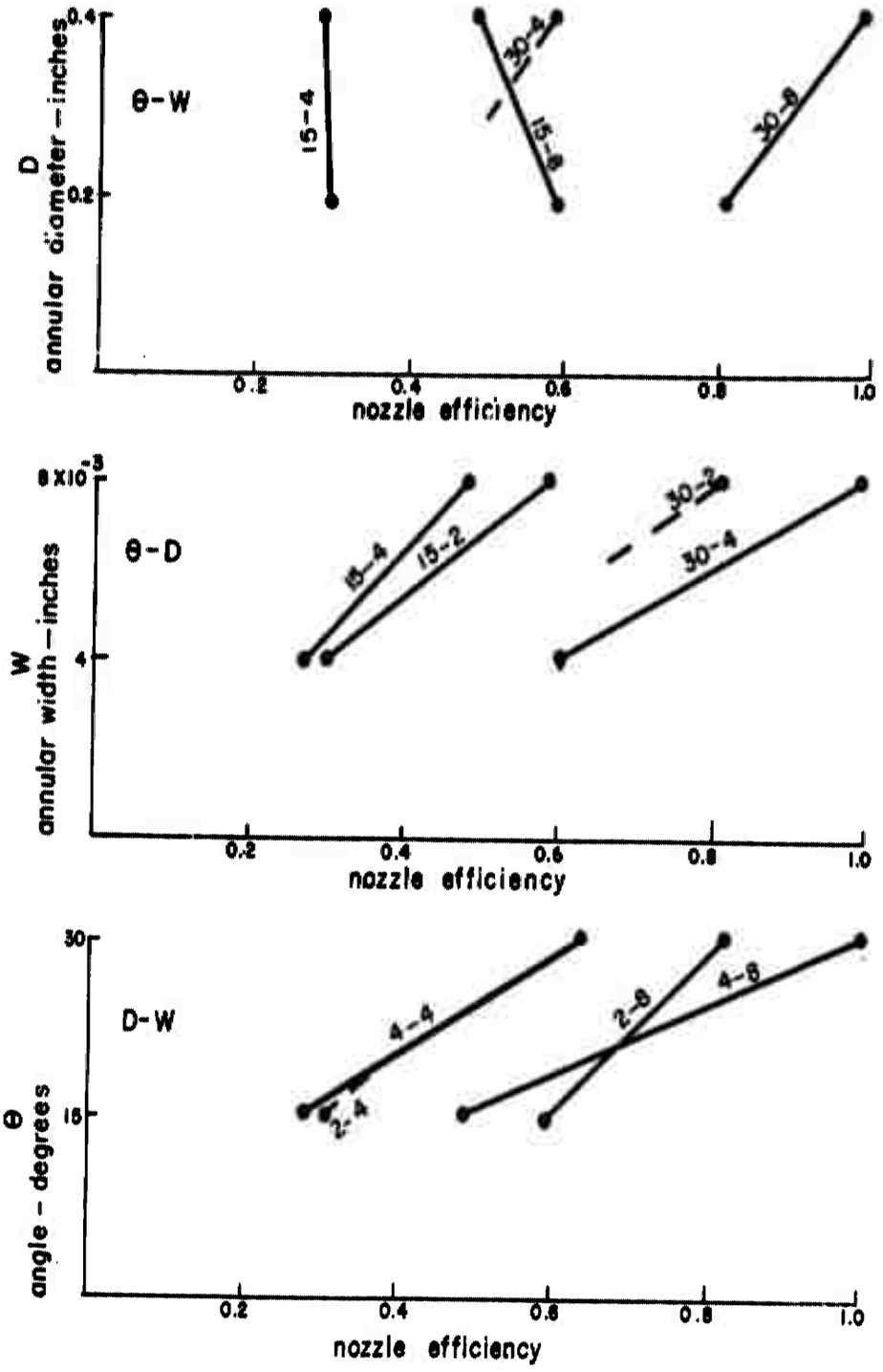

Figure 19. Relationship Of Nozzle Efficiency Values To Nozzle Design Features.

Although the velocity gradients in the sheet during the expansion of the jet to the point of breakup cannot be determined, it is reasonable to suppose that they are some function of the initial velocity gradients existing at the nozzle. An average value for the velocity gradients in the nozzle can be estimated where "average value" is defined as that value of velocity gradient which can account for the energy loss in the nozzle as the liquid gains kinetic energy. In the nozzle,

$$PE = KE + D_\eta \qquad (11)$$

where PE = potential energy of the liquid per unit volume

KE = kinetic energy as liquid leaves the nozzle

D_η = energy loss, during the transformation from potential to kinetic energy, due to viscous shear.

The rate of dissipation of energy within a liquid flowing within fixed boundaries is given by:[10]

$$\eta \int_v \int dv \qquad (12)$$

where $\bar{J} = \bar{\nabla} \times \bar{V}$ $\bar{V}$ = velocity vector, dv = volume element.

Consequently, the rate of dissipation per unit volume is:

$$\omega = \eta \left| (\bar{\nabla} \times \bar{V}) \right|^2$$

Assuming steady flow parallel to the nozzle axis, then

$$\left| \bar{\nabla} \times \bar{V} \right| = \left| \frac{dV_3}{dr} \right|$$

where r = radius vector.

Hence, the average rate of dissipation:

$$\overline{\omega_i} = \eta \left| \frac{dV_3}{dr} \right|^2$$

And the average dissipation in the nozzle per unit volume:

$$D_n = \overline{\omega_n}\, t = \eta \left| \frac{dv_3}{dr} \right|^2 t \qquad (13)$$

where t = average time for a unit volume to flow through the nozzle,

$$t = l/\bar{v}$$

where l = length of nozzle orifice

$\bar{v}$ = average velocity of liquid defined by:

$$\bar{v} A_{\perp} = Q$$

$A_{\perp}$ = cross-sectional area of nozzle

Q = volume flow rate.

Using (11), this average initial velocity gradient could then be calculated for each nozzle:

$$\left[\frac{\left(P - \frac{1}{2} \rho \bar{v}^2 \right) \bar{v}}{\eta l} \right]^{\frac{1}{2}} = \left(\frac{d \bar{v}_s}{dr} \right) \qquad (14)$$

where P = gage pressure in dynes/cm^2 in the liquid reservoir at the nozzle entrance.

Critical energy and dissipated energy in the free jet are an increasing function of this average initial velocity gradient. Curves are drawn in Figure 20 as linear approximations. Assuming linearity, it follows:

$$D = \alpha KE + C \qquad (15)$$

D = dissipated energy

KE = critical energy

C, α = constants

A plot of dissipated energy versus critical energy indicates c = 0, and the dissipated energy is an approximately linear function of the critical energy. See Figure 21.

Rewriting (15): $\int F - d\mu = \alpha \frac{1}{2} \rho \bar{v}^2$

where $\alpha = 0.040 \pm 0.016$ average deviation

The average nozzle efficiency can be written:

$$\bar{E} = 1 - \frac{\alpha}{\sin^2 \Theta} \qquad 15^\circ \leq \Theta \leq 30^\circ \qquad (16)$$

This shows that the average nozzle efficiency for the jet in the critical state is a function of Θ alone for this range of Θ since R is independent of Θ. Two values of E calculated by (16) agree with the average value of the efficiencies of all nozzles with the same nozzle angle Θ.

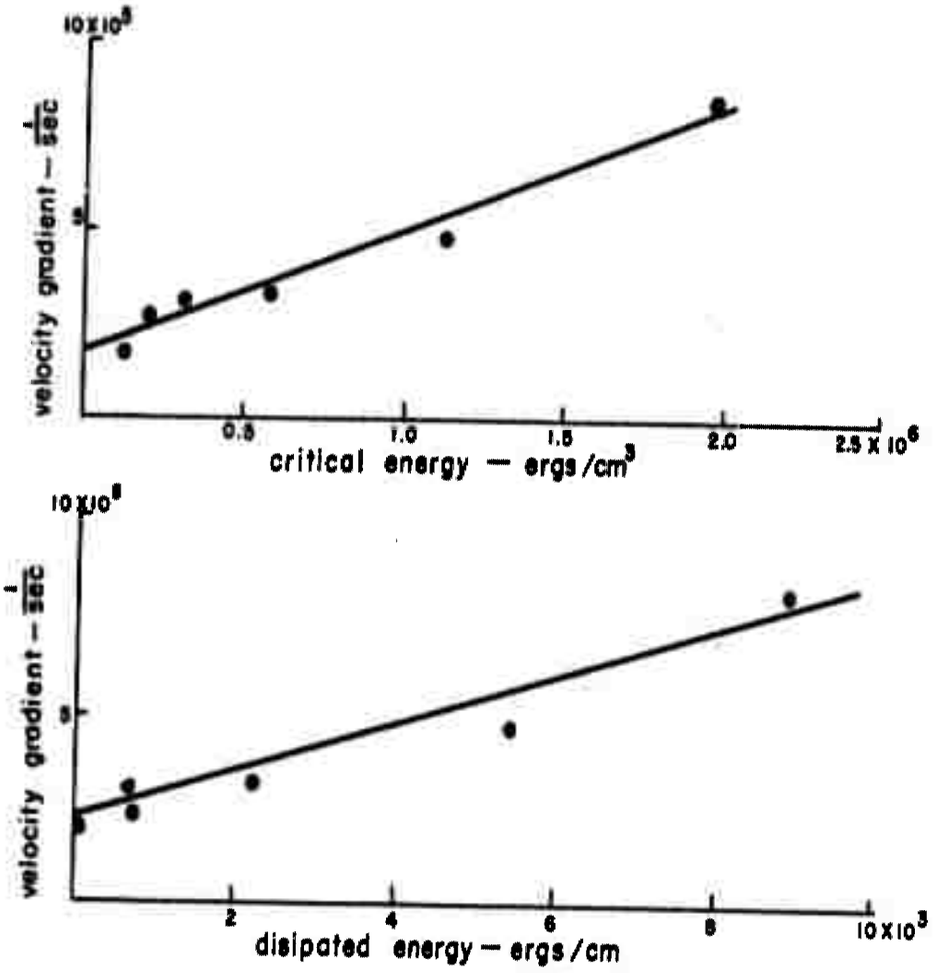

Figure 20. Critical And Dissipated Energy As A Function Of Initial Velocity Gradient.

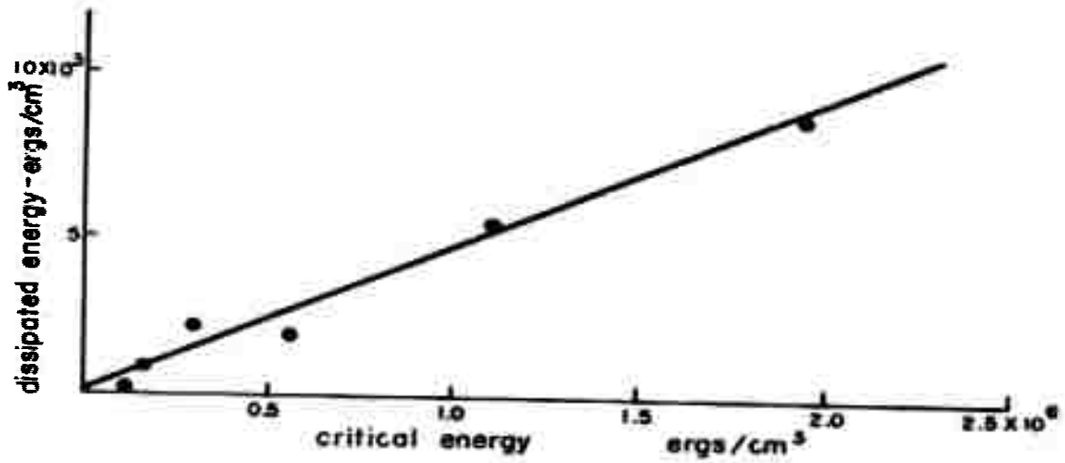

Figure 21. Dissipated Energy vs. Critical Energy

θ	$E_{(16)}$	$\bar{E}$
15	.45	.41
30	.84	.82

The fluctuation of the efficiencies about the average for a given angle are reflected in the spread of the value α. This spread may be due to the variation in velocity gradient for a given angle. The individual efficiencies seem to decrease with an increase in both initial average velocity gradient and initial average velocity. These latter two quantities are of course not independent of each other. See Figure 22. Nozzle efficiency as a function of angle can be considered from two points of view. For two nozzles with different angles but equal annular diameter and annular width, the initial energy available for work in the direction normal to the nozzle axis under critical conditions is of the same order of magnitude. The total kinetic energy, however, varies inversely as $\sin^2\theta$. Since the energy dissipated is directly proportional to the total kinetic energy, the efficiencies of the two nozzles differ, due to the increased energy dissipation, i.e,

$$\tfrac{1}{2}\rho\bar{v}_1^2\sin^2\theta = \tfrac{1}{2}\rho\bar{v}_2^2\sin^2\theta_2 = A$$

A = constant

$$E = 1 - \frac{\int F\,dx}{\frac{1}{2}\rho\bar{v}^2\sin^2\theta} = 1 - \frac{\int F\,dx}{A}$$

$$\int F\,dx = \alpha\left(\tfrac{1}{2}\rho\bar{v}^2\right) = \frac{\alpha A}{\sin^2\theta}$$

Or, secondly, if the annular width could be varied in such a way as to produce the same critical energy for two different angle values, then the dissipation would be fixed and the increased efficiency for the nozzle with the larger angle would reflect the greater availability for work in storing surface energy. Hence, the actual stored surface energy is increased as well as the efficiency of the process involved in its storage.

$$\tfrac{1}{2}\rho\bar{v}_1^2 = \tfrac{1}{2}\rho\bar{v}_2^2 = B$$

B = constant

$$B\sin^2\theta = SE + D$$

SE = surface energy

$D = \int F\,dx$ = constant

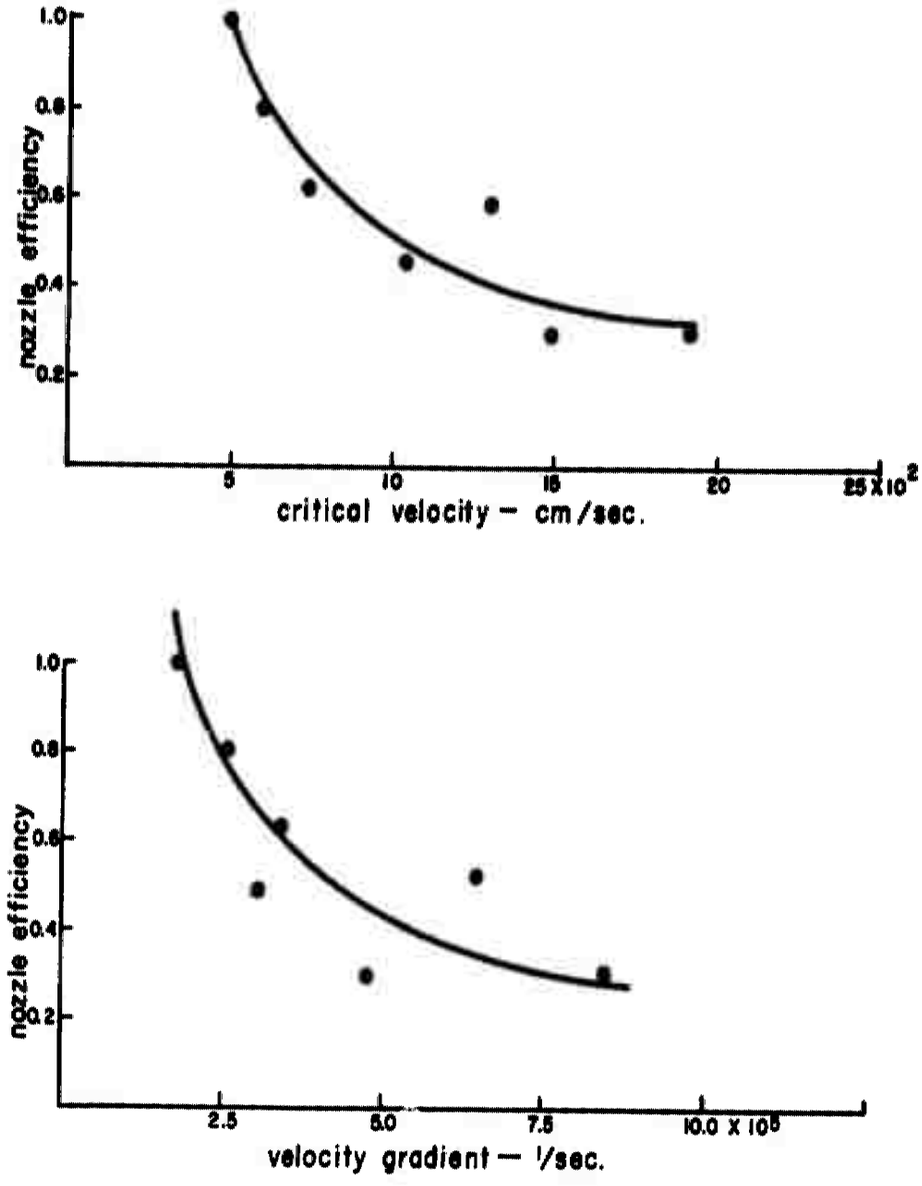

Figure 22. Relationship Of Critical Velocity and Velocity Gradient To Nozzle Efficiency.

and the difference in surface energy for the two nozzles, ΔSE, is given by:

$$\Delta SE = B(\sin^2\theta_1 - \sin^2\theta_2) \qquad \theta_1 > \theta_2$$

Reynold's Numbers for the eight nozzle combinations varied from 566 to 2594, and there was no apparent correlation between R_e and the various measured values.

An empirical examination was made of the total efficiency of each nozzle, defined as the ratio of surface energy per unit volume at point of breakup to the initial potential energy per unit volume in the nozzle, i.e., the pressure

$$E_t = \frac{2\sigma/T_2}{P}$$

where E_t = total efficiency

T_2 = apparent sheet thickness at breakup

σ = surface tension

P = pressure in dynes/cm^2 in the nozzle at the critical state of the jet.

This empirical treatment shows that $E_t = \frac{1}{3}\sin^2\theta \pm 15\%$ a.d.

for all nozzles. Values of E_t were:

	15°	30°
E_t	.02	.08 ± 15%

Summary of Part 3

(1) The average kinetic energy, defined by $\frac{1}{2}\rho \bar{v}^2$, where $\bar{v} = \frac{Q}{A_\perp}$, Q = volume flow rate, $A_\perp$ = cross-sectional area of nozzle perpendicular to flow, necessary to produce breakup of an expanding conical jet of water, was measured for eight hollow conical nozzles differing in annular width, annular diameter and angle. With any two of these design features as parameters, this "critical energy" was a decreasing function of the third nozzle dimension.

(2) The apparent sheet thickness, based on a uniform sheet cross-section, was measured by a velocity determination of the jet at point of breakup. This was found to vary slightly with the various design features, decreasing with angle and increasing with diameter and annular width. Average thickness for all the jets was 3.49×10^{-3} cm $\pm$ 20%.

(3) The energy dissipated in transforming kinetic energy into surface energy and the critical energy were both increasing functions of the average initial velocity gradient. The ratio of these two energies was a constant for all nozzles within 40%. The average "nozzle efficiency", for a given angle value, agreed within 8% of the value calculated using the constant "Nozzle efficiency" is defined as the ratio of the change in surface energy of the jet per unit volume as it expanded to the point of breakup to the kinetic energy due to the initial radial component of velocity.

(4) For a given angle, there was a spread in values of nozzle efficiency. In general, nozzle efficiencies increased with angle and annular width, the dependence on the former being dominant.

(5) There was indication of a correlation between nozzle efficiency and both average initial velocity gradient and critical velocity. This could explain the spread of values about the average value for a given nozzle angle.

(6) The total efficiency of each nozzle, defined as the ratio of surface energy per unit volume at breakup to the potential energy per unit volume in the nozzle, i.e., the pressure, could be expressed empirically by:

$$E_t = \frac{1}{3} \sin^2\theta$$

where θ = nozzle half angle for the $15^\circ \leq \theta \leq 30^\circ$ range

4. A SIMPLIFIED MODEL FOR THE ENERGETICS INVOLVED IN THE BREAKUP OF AN EXPANDING CONICAL JET

There is much work in the literature on liquid jet phenomena both of experimental and theoretical nature. Investigations date back to the latter half of the 19th Century when such workers as Rayleigh, Plateau, Savart and others considered the problem of instability of a solid jet. In Rayleigh's classic paper[1] instability is discussed from two points of view. The first approach considers the disintegration of an infinite cylinder as a result of initial surface disturbances building up under influence of surface tension and disrupting the mass in such a way as to decrease the original surface area. The other point of view is concerned with instability of a jet in a frictionless fluid medium,

1/ See Bibliography

Dynamic reaction of the air surrounding a solid jet was investigated by Weber[3,4] who found that air friction decreased the wave length of oscillations and shortened the breakup distance. Castleman[5] cites air reaction as the primary cause for atomization in solid injection work, and experiments conducted by D. W. Lee[6] on fuel jets showed that increased atmospheric pressure increased the disruption of a jet.

It would appear that the dynamics of jet action involve surface tension, viscosity, and reaction of the atmosphere surrounding the jet, and any investigation of jets, such as stability, kinematic analysis, or energy measurements should take into consideration these factors.

The hollow conical jet is discussed by several authors. Hodgkinson[7] has made a theoretical analysis of the shape of a conical jet as controlled by surface tension. Effects of viscosity and any atmospheric reaction were not taken into account. The justification for neglecting air resistance was a low jet velocity. He found, for low jet velocities, that the theoretical shape of the jet agreed reasonably well with that obtained experimentally for water. F. H. Garner, A. H. Nissan, G. F. Wood[8] used the conical jet to measure the smallest initial value of kinetic energy necessary to shatter a jet. This energy they termed "rupture strength", and found its value to be a linear function of surface tension. It was found to be independent of viscosity and Reynold's Number.

In the present discussion, an attempt is made to develop a simplified model for the energetics involved in the breakup of an expanding conical jet. The effects of viscosity and atmospheric reaction will be included in the model, since theory and experimental work indicate the influence of these factors on jet action.

A diverging, hollow conical sheet of liquid issuing from an annular orifice will possess energy in three forms. It will have potential energy with respect to some reference plane in the gravitational field, it will possess surface energy, and finally it will have kinetic energy, all of which can be expressed in terms of a unit volume. The subsequent dynamics of the jet will depend on the way the various energy components are partitioned and the nature of the forces acting in the system. The "system" is comprised of the liquid jet and the surrounding medium into which the jet issues. In this discussion, the medium is air at atmospheric pressure. Stored energy due to shear stress, such as may be present in visco-elastic systems, will be neglected.

At the orifice of a diverging conical nozzle where the effects of hydrostatic pressure of the closed hydraulic system are zero, there are four forces acting in the liquid-air system:

1. Surface tension forces,

2. Gravitational forces,

3. Frictional resistance of the air parallel to the motion of the jet surface,

4. Frictional forces in the jet itself due to the viscosity of the liquid and any velocity gradients present.

The space integrals of these forces will determine the nature of the change in the partitioning of the initial energy of the system.

The initial energy per unit volume of liquid at the orifice is partitioned in the following way:

1. Surface energy:

$$S = \frac{2\sigma}{T_1} \qquad (1)$$

where S = surface energy per unit volume,

σ = surface tension of moving surface,

T_1 = initial film thickness

This is true for an adiabatic process. For an isothermal process, an additional term in total surface energy is required to account for heat transfer, i.e.,

$$S_T = \sigma - T_a \frac{d\sigma}{dT_a} \qquad \text{Reference (9)}$$

where T_a = absolute temperature.

Adiabatic conditions will be assumed in this discussion.

2. Kinetic energy:

$$KE = \frac{1}{2}\rho \bar{v}_1^2 \qquad (2)$$

where $\bar{v}_1$ = initial average liquid velocity.

ρ = liquid density.

3. Gravitational potential:

$$G = \rho g h$$

where g = gravitational constant.

h = height above an arbitrary reference plane.

The energy per unit volume at any point in the jet in the steady state will be a function of the initial energy and space integrals of force acting during the time an element of jet has been in motion. If the energy per unit volume of the jet can be measured at any subsequent time after the volume element has left the nozzle, then something of the nature of the forces at work in the system can be deduced.

The final energy per unit volume of the jet, taken at the point of breakup for the jet in the "critical state", consists of two terms, if the reference plane for the gravitational potential is at the point of breakup. These terms are:

1. Surface energy:

$$S_f = \frac{2\sigma}{T_2} \qquad (3)$$

where T_2 = final film thickness.

2. Kinetic energy:

$$KE = \frac{1}{2}\rho \bar{v}_f^2 \qquad (4)$$

where $\bar{v}_f$ = final average jet velocity.

The difference between the sums of initial and final energies constitutes dissipation per unit volume of the jet as it expands from the nozzle to the point of breakup. This dissipation can be separated into two terms:

1. Dissipation in the liquid as a result of velocity gradients.

A precise evaluation of this term would require knowledge of velocity gradients as a function of spacial coordinates and time and a knowledge of the boundary conditions in the free jet. Since this knowledge is lacking, an admittedly over-simplified but perhaps useful model will enable the dissipation to be discussed in an empirical way using gross averages. Assume that the velocity gradients, initially present in the liquid sheet or set up and maintained by the interaction of the sheet and the atmosphere, are entirely confined to a boundary layer on the external surface of the sheet. The inner layer of the sheet, whose thickness is large compared to the boundary layer, will have a flat velocity profile. The boundary layer will have a linear velocity profile. See Figure 23.

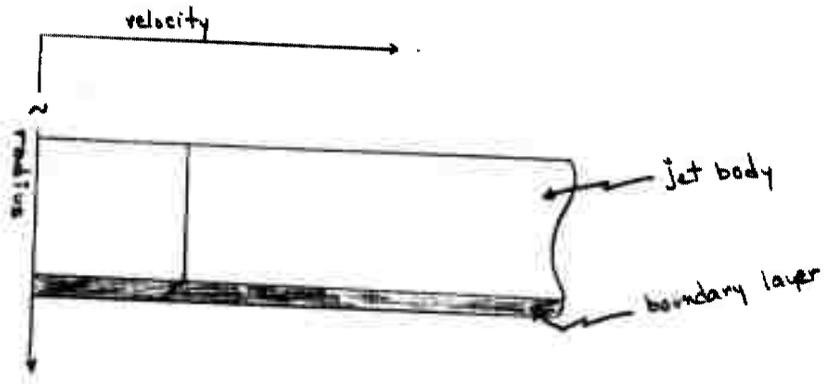

Figure 23

The velocity gradient set up in the boundary layer, $\frac{\bar{dv}}{dr}$, is due to a drag force acting on the outside sheet surface by the atmosphere and the relative sheet-atmosphere velocity. Call this average force over the entire length of the jet acting on a unit area, $\bar{f}$.

Then

$$\bar{f} = 2\pi r \, dl \, \eta \, \frac{\bar{dv}}{dr} \qquad (5)$$

But this force reacts on the jet body tending to retard its motion, and the loss in kinetic energy of the jet body will appear as dissipation by the production of heat in the boundary layer. Hence, the dissipation per unit volume of jet, D, during the jet motion from the nozzle to the point of instability, is given by the space integral of this force per unit volume over the distance, l,

$$D = \frac{\int\int 2\pi r \, dl \, \eta \, \frac{\bar{dv}}{dr} \cdot dl}{\int 2\pi r \bar{T} \, dl} \qquad (6)$$

where $\bar{T}$ = average sheet thickness independent of l,

Hence

$$D = \frac{\eta \left(\frac{\bar{dv}}{dr}\right) l}{\bar{T}} \qquad (7)$$

Using equation (13), Part 3, another expression for the dissipation per unit volume can be written in terms of the average velocity of the jet body, $\bar{v}$, over the length, l.

$$D_i = \eta \left(\frac{\bar{dv}}{dr}\right)^2 \frac{l}{\bar{T}} \qquad (8)$$

Equating this to equation (7)

$$\frac{\bar{dv}}{dr} = \frac{\bar{v}}{\bar{T}} \qquad (9)$$

2. Kinetic energy imparted to air by interaction with a unit volume of jet, W_a.

Equating initial energy and final energy of the jet per unit volume at point of breakup gives:

$$\frac{1}{2}\rho \bar{v}_0^2 + \frac{2\sigma}{r_1} + \rho g h = \frac{1}{2}\rho \bar{v}_f^2 + \frac{2\sigma}{r_2} + \eta \frac{d\bar{v}}{dr}\frac{\ell}{\bar{v}} + W_a/\text{unit vol liquid} \quad (10)$$

The work performed by the jet on the air, W_a, is given by:

$$W_a = \int \bar{f} \cdot d\ell = \iint 2\pi r \, dl \, \eta \frac{d\bar{v}}{dr} d\ell \quad (11)$$

This equals the dissipation in the jet, as expressed in equation (6) and the kinetic energy imparted to the air equals the dissipation in the jet.

The average velocity gradient in the jet is a function of the velocity gradient initially present in the jet as it leaves the nozzle and the gradients set up in the jet as a result of the outside jet layers interacting with the atmosphere. If a velocity gradient exists in the jet initially, and the outside jet layer has zero intial velocity, then the force tending to accelerate the slower moving jet layer, $\bar{F}$, is given by

$$\bar{F} = \eta \left(\frac{d\bar{v}}{dr}\right) 2\pi r \, dl$$

This force will be initially unopposed since the reaction of the air on the jet results from the jet-air relative velocity. As the outside layer gains in velocity, it will experience a retarding force because of its interaction with the air, and this force will tend to retard the decrease in the velocity gradient initially present in the jet.

Hence,

$$\int \bar{f} \cdot d\ell < \iint \eta \frac{d\bar{v}}{dr} 2\pi r \, dl \, dl \quad (12)$$

since some energy is dissipated in the jet while the outside layer is being accelerated to the point where $\bar{v}_f$ is established, $\frac{d\bar{v}}{dr}$ having been defined as that value of velocity gradient necessary to account for the total energy dissipation in the jet. In other words, $\bar{v}_f$ alone does not account for this average velocity gradient, but the latter is also a function of the initial velocity gradient.

To simplify the treatment, equation (11) will be assumed, since estimation of the degree of inequality has not as yet been made.

Hence, equation (11) expressed in terms of a unit volume of liquid equals (7), and (10) may be rewritten:

$$\frac{1}{2}\rho\bar{v}_0^2 + \frac{2\sigma}{r_1} = \frac{1}{2}\rho\bar{v}_f^2 + \frac{2\sigma}{r_2} + 2\eta\left(\frac{dv}{dr}\right)\frac{l}{\bar{v}_f} \qquad (13)$$

where gravity is neglected.

Rearranging,

$$\frac{\frac{1}{2}\rho\bar{v}_0^2}{\sigma} = \left(\frac{2}{\sigma}\frac{l}{\bar{v}_f}\frac{d\bar{v}}{dr}\right)\eta + \frac{1}{2}\rho\bar{v}_f^2 + 2\left(\frac{1}{r_2} - \frac{1}{r_1}\right) \qquad (14)$$

The empirical equation reported in Part 2 relating the critical energy with viscosity and surface tension may be compared with (13). For a viscosity range of $0 < \eta < 5$ c.p. it was of form:

$$\frac{\frac{1}{2}\rho\bar{v}_0^2}{\sigma} = k_1\eta + c_1 \qquad (15)$$

For a viscosity range $5 \leq \eta < 45$ c.p.

$$\frac{\frac{1}{2}\rho\bar{v}_0^2}{\sigma} = k_2\eta' + c_2 \qquad (16)$$

where K_1, k_2, c_1, c_2 are constants.

and $\eta' = \eta - 5$. c.p.

Rewrite equation (13)

$$\frac{\frac{1}{2}\rho\bar{v}_0^2}{\sigma} = K\eta + A$$

where

$$K \equiv \frac{2l}{\sigma\bar{T}}\frac{d\bar{v}}{dr} \quad \text{and} \quad A \equiv \frac{\frac{1}{2}\rho\bar{v}_f^2}{\sigma} + 2\left(\frac{1}{r_2} - \frac{1}{r_1}\right) \qquad (17)$$

Assuming K, A are independent of viscosity for each viscosity range, then

$$\left.\begin{aligned} K &= k_1 \\ A &= c_1 \end{aligned}\right\} \text{ for } 0 < \eta < 5$$

$$\left.\begin{aligned} K &= k_2 \\ 5K+A &= C_2 \end{aligned}\right\} \text{ for } 5 < \eta < 45 \qquad (18)$$

A single experiment has been performed to check this relationship. Two liquids were used for the two viscosity ranges. The first was a 10% ethyl alcohol and water solution with a viscosity of 2 cp and a surface tension of 52 dynes/cm. The second solution, 50% sucrose and water, had a viscosity of 10 cp and a surface tension of 63.0 dynes/cm. The two jets were photographed from the subcritical up through the critical stage. In the subcritical velocity region the expanding conical jet reaches a maximum diameter consistent with the initial kinetic energy, and then is contracted to a solid stream with circular cross-section.

By using the equation of continuity, the average velocity at the point of contraction can be calculated from a measurement of the cross-sectional area. The distance the jet travels prior to the point of collapse is also measured. An expression can be written for the average force per unit volume acting on the jet.

$$\bar{f}_r = \frac{(\rho \bar{v}_0 - \rho \bar{v}_f)\,\bar{v}}{l} \qquad (19)$$

where $\bar{f}_r$ = drag per unit volume

v_0 = initial velocity

v_f = velocity at point of contraction

l = measured distance along jet to point of contraction from nozzle.

$\bar{v}$ = average velocity over the distance, .

In order to calculate $\bar{f}_r$, a value of $\bar{v}$ must be known.

It was assumed that the instantaneous force per unit volume acting on the jet was related to the instantaneous velocity by the following equation:

$$f = -\beta v^2 \qquad (20)$$

where f = instantaneous force per unit volume,

v = instantaneous velocity,

B = factor of proportionality, assumed constant.

Integration and rearrangement give:

$$v = \frac{v_0 \rho}{B t v_0 + \rho}$$

where t = time

= density of liquid

$$l = \frac{\rho}{B} \ln\left[\rho + B v_0 t\right] - \frac{\rho}{B} \ln \rho$$

$$\bar{v} = \frac{\left[\rho v_0 \ln\left\{\left|\rho + \left(\frac{v_0 \rho - v\rho}{v}\right)\right|\right\} - \rho v_0 \ln \rho\right] v}{v_0 \rho - v\rho} \qquad (21)$$

$$l = \frac{\rho}{B} \ln\left[\rho + B v_0 \left(\frac{v_0 \rho - v\rho}{v v_0 \rho}\right)\right] - \frac{\rho}{B} \ln \rho \qquad (22)$$

Using (21), fair consistency in the measured value of B for the jets having various initial velocities in the subcritical region justified the assumption of Equation (19). This argument was applied to the jets in the critical region, and the drag was calculated using (18). Using this value of force of interaction between the jet and the air, the dissipation was then calculated according to (11) and (7).

$$2 \int \bar{f}_v \cdot dl = \frac{2l}{T} \frac{d\bar{v}}{dr} \eta \qquad (23)$$

A in (16) is known from the final velocity and the diameter of the jet at point of breakup.

$$v_f \pi d T_2 = Q \qquad (24)$$

where Q = volume flow rate,

d = jet diameter at point of breakup,

v_f = velocity of jet at breakup,

Hence, the constants K and A in (17) can be calculated and compared with their empirical counterparts reported in Part 2.

	Calculated	Empirical
Ethanol		
K	1.00×10^4	k_1 0.4×10^4
A	0.3×10^4	c_1 1.3×10^4
Sucrose		
K	1.00×10^4	k_2 1.1×10^4
A+5K	6.5×10^4	
A	1.5×10^4	c_2 3.3×10^4

Another method of computing the energetics involved in the breakup of the conical jet involves the horizontal component of motion, x axis in Figure 24.

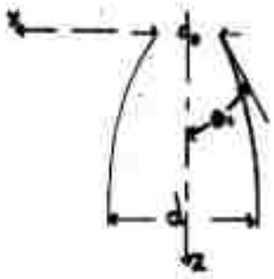

Figure 24.

The jet emerges from the nozzle at the nozzle angle, θ_0. The surface tension opposes the horizontal motion, decreasing the x component of velocity and θ. At the point of breakup in the "critical state" the horizontal velocity is zero and the jet flows parallel to the z axis. At this point in the jet motion, the kinetic energy due to the initial component of velocity along x has been expended in storing surface energy and in doing dissipative work. There is no residual kinetic energy term for this component.

The x component of dissipation may be written from (22)

$$2\int \bar{f}_x \cdot dx = \left(2\,\frac{l}{\pi}\,\frac{d\bar{r}}{dx}\right)_x \eta \qquad (24)$$

where $\bar{f}_x$ = average drag component along x.

$\frac{2l}{\pi}\left(\frac{dr}{dx}\right)_\eta$ = portion of total dissipated energy due to x component of motion.

The integration is over the total horizontal distance traveled by a unit volume of jet, i.e., $d - d_o$ in Figure 23.

The jet surface will make some average angle, $\bar{\theta}$, with the jet axis such that:

$$\bar{f}_x = \bar{f}_v \sin\bar{\theta} \qquad (26)$$

The energy equation for this component is

$$\frac{1}{2}\rho \bar{v}_o^2 \sin^2\theta_o + \frac{2\sigma}{r_1} = \frac{2\sigma}{r_2} + \left(\frac{2l}{\pi}\frac{d\tau}{dr}\right)_x \eta \qquad (27)$$

Hence, an equation for the horizontal component analogous to Equation (13) may be written in form

$$\frac{\frac{1}{2}\rho \bar{v}_o^2 \sin^2\theta_o}{\sigma} = \frac{2\sigma}{\sigma}\int_{d_o}^{d} \bar{f}_v \sin\bar{\theta}\, dx + 2\left(\frac{1}{r_2} - \frac{1}{r_1}\right) \qquad (28)$$

where θ_o = initial jet angle, i.e., nozzle half angle.

and $$2\int_{d_o}^{d} \bar{f}_v \sin\bar{\theta}\, dx = \left(\frac{2l}{\pi}\frac{d\tau}{dr}\right)_x \eta$$

Let

$$K_x \equiv \left(\frac{1}{\sigma}\,\frac{2l}{\pi}\frac{d\tau}{dr}\right)_x$$

$$A_x \equiv 2\left(\frac{1}{r_2} - \frac{1}{r_1}\right)$$

Rewriting (27)

$$\frac{\frac{1}{2}\rho \bar{v}_o^2 \sin^2\theta_o}{\sigma} = K_x \eta + A_x \qquad (29)$$

The empirical data of Part 2 can be plotted in terms of the initial kinetic energy due to the component of velocity. For a viscosity of

$0 < \eta \leq 5$ cp, the empirical equation is of form:

$$\frac{\frac{1}{2}\rho \bar{v}_o^2 \sin^2\theta_o}{\sigma} = A_{1x}\eta + C_{1x}$$

For a viscosity range $5 < \eta < 45$ cp

$$\frac{\frac{1}{2}\rho \bar{v}_o^2 \sin^2\theta_o}{\sigma} = A_{2x}\eta' + C_{2x}$$

where, as before,

$K_{1\gamma}$, $K_{2\gamma}$, $C_{1\gamma}$, $C_{2\gamma}$ are constants

and $\eta' = \eta - \sigma$

Again, as in the total energy relationship, assuming K_γ and A_γ are independent of viscosity for a given viscosity range,

$$\left.\begin{aligned} K_\gamma &= B_{1\gamma} \\ A_\gamma &= C_{1\gamma} \end{aligned}\right\} \text{ for } 0 < \eta \leq 5 \text{ c.p}$$

and

$$\left.\begin{aligned} K_\gamma &= B_{2\gamma} \\ A_\gamma + \sigma K_\gamma &= C_{2\gamma} \end{aligned}\right\} \text{ for } 5 < \eta < 45 \text{ c.p.}$$

$\bar{\theta}$ in (26) can be approximated geometrically. The jet will have a shape similar to that in Figure 25.

Figure 25.

such that Tan $\bar{\theta} = R_c/L$

where R_c = ritical radius

L = distance to point of breakup from the nozzle along the jet axis.

$\bar{\theta} \cong \theta_c/2$ for both the ethanol and sucrose jets.

Using this value of $\bar{\theta}$, the average horizontal drag force can be calculated from (26), and k_γ, A_γ may be computed and compared with the empirical values.

	Calculated		Empirical
Ethanol			
	k_x 1.85×10^2	k_{1x}	1.43×10^2
	A_x $.96 \times 10^2$	c_{1x}	3.5×10^2
Sucrose			
	K_x 2.10×10^2	k_{2x}	2.8×10^2
	A_x 1.30×10^2		
	A_x+5K_x 11.80×10^2	c_{2x}	10.5×10^2

Discussion and Summary of Part 4.

There is "order of magnitude" agreement between the empirically determined quantities and calculated results based on the simplified model and the experiment performed to measure the energy dissipation. The error involved in the simplifying assumptions used in developing the model and in making the calculations cannot be estimated without further work. For example, neglecting the initial velocity gradient in the jet in computing the jet-air interaction introduces an error which might be capable of evaluation if a series of tests was performed at sub-atmospheric pressures. Qualitatively, neglecting the initial velocity gradients would have a tendency to increase K and K_x over their true value, and this effect should be more pronounced for the lower viscosity solutions. A second assumption that K and A are independent of viscosity in the two viscosity ranges again requires further experimental work for its verification. From these preliminary results, it appears that this assumption is better justified in the case of the sucrose solution than for the ethanol solution in the low viscosity range. Qualtitatively this is reasonable. The empirical straight-line relationships (15) and (16) were approximations to a continuous function over the entire viscosity range, of general form.

$$\frac{\frac{1}{2}\rho \bar{v}_0^2}{\sigma} = k\eta + c$$

where $K = k(\eta)$

c = constant.

The transition region between the two straight-line relationships, where k is approximately constant, involves a change in slope with viscosity. $d\%/d\eta$ had a maximum value fairly well defined at $\eta = 5$ cp. The accuracy of the data did not, however, preclude a slight variation in k

with η for lower viscosity values. The sucrose solution falls on that region of the curve where the slope was less sensitive to a change in viscosity.

The absolute energy balance for both the ethanol and sucrose solutions using the total energy equation (13) was high on the "work done" side by 60%. The lack of agreement between the initial and final energy values is probably due in part to ignoring the effect of initial velocity gradient on the drag, thus increasing the value of the dissipation term. Using the x - component equation (27) the balance is better, being 17% and 7% for ethanol and sucrose respectively. Here, the excess energy appears on the "initial" side of the equation. An explanation for this reversal in error trend over the total energy equation probably lies in the evaluation of the surface energy at point of breakup. This energy is insignificant in the total energy balance where residual kinetic energy and dissipation terms are larger by a factor of 100. For the x - component balance it becomes significant.

The surface energy was calculated on the assumption of a uniform annular cross section at the breakup point of the jet. This assumption is more justifiable in the case of the higher viscosity sucrose jet than for ethanol, where surface irregularities are more pronounced. The surface energy per unit volume at the point of breakup is given by:

$$2\sigma/T_2$$

where σ = surface tension,

T_2 = jet sheet thickness, assumed uniform.

T_2 was calculated from the equation of continuity and the surface energy computed from this "apparent" thickness. The values for ethanol and sucrose are given below:

	Apparent thickness	Initial thickness
Ethanol	23.0×10^{-3} cm.	22.0×10^{-3} cm.
Sucrose	14.7×10^{-3}	22.0×10^{-3}

The apparent thickness of the ethanol jet indicates a decrease in surface energy per unit volume as the jet expands. This is not physically reasonable. An "effective" thickness can be calculated, using equation (26) which would afford a better approximation of the stored surface energy, i.e., better indicate the increased surface area per unit volume.

These values are found to be:

	Ethanol	Sucrose
Effective thickness	9.9×10^{-3} cm.	6.1×10^{-3} cm.

The values obtained for the partitioning of energy in the two jets are given in Table III.

TABLE III

Solution	Total Energy	X-Component	
Ethanol		"Effective T_2"	"Apparent T_2"
Initial Kinetic Energy	0.617×10^6 ergs/cm^3	23,700	23,700
Residual Kinetic Energy	0.163×10^6	0	0
Dissipated Energy	1.120×10^6	17,900	17,900
Final Surface Energy	10,527	10,527	4,900
Increase in Surface Energy	5,780	5,800	-200
Sucrose			
Initial Kinetic Energy	4.823×10^6 ergs/cm^3	140,000	140,000
Residual Kinetic Energy	0.740×10^6	0	0
Dissipated Energy	6.760×10^6	125,200	125,200
Final Surface Energy	20,527	20,527	8,600
Increase in Surface Energy	8,300	14,800	3,500

Several a priori hypotheses were suggested in Part 2 to explain the dependence of the "critical energy" on viscosity,

1. Increased jet stability induced by an increase in the viscosity of the liquid, allowing more work to be done in storing surface energy and against frictional forces.

2. Increased dissipation as a result of increased viscosity.

The data in Table III indicate that both these effects exist. The greater increase in surface energy of the higher viscosity sucrose solution results from a smaller sheet thickness of the jet at breakup since the surface tensions of the two liquids are approximately equal. And secondly, the dissipation of energy in the two jets is approximately proportional to the respective viscosities. Using the "effective thickness" values, 75% of the initial energy available for work in storing surface energy is expended in overcoming dissipative loss in the case of the ethanol jet, and 88% is similarly expended by the sucrose jet.

The "nozzle efficiencies", defined as the ratio of the increase in surface energy to the initial kinetic energy available for the increase, are:

Ethanol 24.4%
Sucrose 10.5%

On the basis of efficiency, the relative gain in stored surface energy effected by increasing the viscosity of the liquid is counteracted by a greater energy dissipation.

BIBLIOGRAPHY

1. "Instability of Jets" Lord Rayleigh Lond. Math. Soc. Vol. 10, 1878

2. "Determination of the surface tension of water by the Method of Jet Vibration" Niels Bohr Phil. Trans. Roy. Soc. Vol. 209, 1909

3. "Zum Zerfall eines Flussigkeitsstrahles" Weber, Von Constantin Zeit Fur Ange Math Vol. 11, 1921

4. "Atomization of Liquid Jets and Droplets" Thomas Baron Tech. Report #4 Eng. Exp. Station U. of Illinois, Feb. 1949

5. "Mechanism of Atomization Accompanying Solid Injection" Castleman, R.A.N.A.C.A. Tech Report #440, 1932

6. "Experiments in the Distribution of Fuel in Fuel Sprays" Lee, D. W. N.A.C.A. Report No. 438, 1932

7. "Control by Surface Tension of a Conical Fluid Sheet Jet" Hodgkinson, J. G. Porton Tech Paper No. 174, 1950

8. "Thermodynamic and Rheological Behavior of Elasto viscous systems under Stress" Garner, F. H.; Nissar, A. H.; Wood, G. F.; Phil. Trans. Roy. Soc. Vol. 243, 1950

9. "Heat and Thermodynamics" M. W. Zemansky McGraw-Hill, 1943

10. "Theoretical Hydrodynamics" Milne - Thomson, L. M., MacMillan Co., N. Y., 1950

GLOSSARY OF SYMBOLS

ρ	liquid density
$\bar{v}_c$	critical liquid velocity
σ	liquid surface tension
η	liquid viscosity
T	jet thickness
$A_\perp$	nozzle orifice cross sectional area normal to stream-lines
E	nozzle efficiency, equals ratio of change in surface energy to initial KE available for conservative work
E_T	total nozzle efficiency, equals ratio of surface energy/unit volume at breakup to initial potential energy/vol. in nozzle
T_a	absolute temperature
$\overline{\frac{dv}{dr}}$	average velocity gradient in liquid
$\bar{T}$	average sheet thickness over jet length
$\bar{f}$	drag force on sheet surface by interaction with atmosphere
$\bar{F}$	average force exerted on outside jet layer by inner jet
$\bar{v}_o$	average initial jet velocity
$\bar{v}_f$	average final jet velocity
$\bar{f}_x$	average force retarding jets motion perpendicular to jet axis
l	length of jet
dl	element of jet length
R	radius of annular orifice
W	annular width of orifice
θ	nozzle half angle
Q	volume flow rate through nozzle

D	dissipated energy in free jet
d	diameter of free jet
KE	initial kinetic energy per unit volume
S	surface energy per unit volume
S_T	total surface energy under isothermal conditions
W_a	energy exchanged to atmosphere by the free jet
PE	potential energy per unit volume of liquid at stagnation point in nozzle
D_n	energy dissipated per unit volume in the nozzle
K_g	kinetic energy imparted to the air by a unit volume of the free jet
$\bar{v}$	average velocity of the jet over the jet length

INTERIM REPORT 30

Distribution List

Copy No.	Addressee
1	Assistant Chief Chemical Officer for BW
* 2	Technical Records
3	Director of Technical Operations
4	Director of Research
5	Director of Development
6	Director of Production Engineering
7	Program Management Office
8, 9	Chief, Assessment Division
10 - 13	Chief, M Division
14	Chief, Plant Design Division
15	Chief, Product Engineering Division
16	Chief, Pilot Plants Division
17 - 19	Commanding Officer, Naval Unit
20 - 36	USAF Development Field Office
37	Commanding Officer, BW Assessment Labs Dugway Proving Ground, Utah
38	Office of the Chief Chemical Officer Research & Development Division Department of the Army Washington 25, D.C. ATTN: BW Liaison Branch
39 - 41	Office of the Chief Chemical Officer Department of the Army Washington 25, D.C. ATTN: PT&I Division (for G-2 and CIA)
42	President, Chemical Corps Board Army Chemical Center, Maryland ATTN: BW Liaison Officer

Distribution List (Cont'd)

Copy No.	Addressee
43	CmlC Advisory Council Army Chemical Center, Maryland
44	Commanding Officer, CmlC Chemical & Radiological Labs Army Chemical Center, Maryland ATTN: Technical Library
45	Commanding Officer, CmlC Medical Labs Army Chemical Center, Maryland
46, 47	Commanding Officer, CmlC Training Command Fort McClellan, Alabama
48	Assistant Secretary for R&D Office of the Secretary of Defense Washington 25, D.C. ATTN: Librarian
49	Lt. Col. L. C. Miller, CmlC Representative for Cml C U. S. Army Standardization Group, U.K. Box 65, USN 100, F.P.O. New York, N.Y.
50 - 55	British Liaison Officer Building No. 1 Army Chemical Center, Maryland
56 - 60	Canadian Army Technical Representative Building No. 1 Army Chemical Center, Maryland
61	Executive Director Operations Research Office Johns Hopkins University 6410 Connecticut Avenue Chevy Chase, Maryland
62	Assistant Secretary of Defense (R&D) Room 3E 1025, The Pentagon Washington 25, D.C. ATTN: Executive Secretary, BW-CW Coordinating Committee

Distribution List (Cont'd)

Copy No.	Addressee
63	Weapons Systems Evaluation Group Office of the Secretary Washington 25, D. C.
* 64	Commanding General CmlC Research and Engineering Command Army Chemical Center, Maryland
* 65	Editorial Section, E&D Branch, RT&O Division
66 - 80	Documents Section, E&D Branch, RT&O Division
81 - 85	Armed Services Technical Information Agency Documents Service Center Knott Building Dayton 2, Ohio

* Copies 2 through 85 are convenience copies. When no longer needed, it is requested that authority for their destruction be obtained from the Documents Section, RT&O Division, Camp Detrick, Maryland.